

Two-cylinder entanglement entropy under a twist

Xiao Chen,^{1,2,*} William Witczak-Krempa,^{3,4,†}

Thomas Faulkner,^{2,‡} and Eduardo Fradkin^{2,§}

¹*Kavli Institute for Theoretical Physics,*

University of California at Santa Barbara, CA 93106, USA

²*Department of Physics and Institute for Condensed Matter Theory,*

University of Illinois at Urbana-Champaign,

1110 West Green Street, Urbana, IL 61801-3080, USA

³*Département de Physique, Université de Montréal,*

Montréal, Québec, H3C 3J7, Canada

⁴*Department of Physics, Harvard University, Cambridge MA 02138, USA*

(Dated: September 30, 2018)

Abstract

We study the von Neumann and Rényi entanglement entropy (EE) of scale-invariant theories defined on tori in 2+1 and 3+1 spacetime dimensions. We focus on spatial bi-partitions of the torus into two cylinders, and allow for twisted boundary conditions along the non-contractible cycles. Various analytical and numerical results are obtained for the universal EE of the relativistic boson and Dirac fermion conformal field theories (CFTs), and for the fermionic quadratic band touching and the boson with $z = 2$ Lifshitz scaling. The shape dependence of the EE clearly distinguishes these theories, although intriguing similarities are found in certain limits. We also study the evolution of the EE when a mass is introduced to detune the system from its scale-invariant point, by employing a renormalized EE that goes beyond a naive subtraction of the area law. In certain cases we find non-monotonic behavior of the torus EE under RG flow, which distinguishes it from the EE of a disk.

CONTENTS

I. Introduction	3
A. Summary of the main results	7
II. General properties of torus entanglement in two dimensions	9
1. Thin slice limit	10
2. Thin torus limit	11
3. Wide torus limit	11
III. Two-cylinder entropy for relativistic free field theory	12
A. The shape dependence	13
B. Thin torus limit & semi-infinite cylinder	15
1. Massive case	18
IV. $z = 2$ free bosons & fermions with a twist	21
A. $z = 2$ free bosons	21
1. Two-cylinder entropy on a cylinder	22
2. Two-cylinder entropy on a torus	25
B. Fermionic quadratic band touching	27
V. Free relativistic theories in $3 + 1$ dimensions	29
A. Massless case	30
B. Massive case	33
VI. Conclusions	35
Acknowledgments	38
A. Useful functions and identities	38
B. Various zeta functions	39
1. Hurwitz zeta function	39
2. Epstein zeta function in $d = 1$	39
3. Epstein zeta function in $d = 2$	40

C. Free boson partition function on the cylinder & torus	42
1. Torus	42
a. Periodic boundary conditions in x & y directions	42
b. Twist boundary condition	43
2. Open cylinder	44
a. Periodic in the y direction	44
b. Twisted boundary condition in the y direction	44
D. Numerical method for calculating EE in free systems	45
1. Free scalar field theory	45
a. Relativistic boson in $2 + 1$ d	46
2. Numerical method for the free Dirac fermion in $2 + 1$ dimensions	47
References	47

I. INTRODUCTION

The entanglement entropy (EE) is a non-local quantity which, when properly treated, can capture the long-distance properties of correlated quantum many-body states and quantum field theories. Given its non-local nature, the behavior of the EE is not as well understood as the correlators of local operators in quantum field theory and, in particular, how they are related to each other. Moreover, due to the non-local character of EE it may capture global properties which may not be accessible by measurements of local operators.

The most complete and detailed understanding to date of the behavior of EE is in $1 + 1$ -dimensional conformal field theories (CFT), which describe the universal behavior of systems at quantum criticality. In these CFTs the von Neumann EE of a single interval in the ground state has a universal logarithmic dependence on the length of the interval. The prefactor of the logarithm yields the central charge c for the underlying CFT, which is the most important quantity to characterize the theory.¹⁻⁴ Furthermore, a related quantity, the mutual information of two disjoint intervals, depends not only on the central charge but also on the operator content of the CFT.⁵ These results connecting the central charge of a CFT to the scaling of the EE suggested that the scaling of EE may be related to definitions of a central charge in higher dimensions,⁶ and to a generalization of the Zamolodchikov

c -theorem⁷ for renormalization group flows.

Much less is known of the behavior of the EE in higher-dimensional field theories. In space dimensions $d > 1$, the von Neumann EE of a local field theory on a finite but macroscopically large region of space satisfies the “area law” and scales with the size of the boundary of the observed region.^{8,9} In a local quantum field theory this behavior, reminiscent of the area law of the Bekenstein-Hawking black hole entropy,^{10,11} is governed by a cut-off dependent non-universal prefactor, and any universal (independent of the UV cutoff) behavior of the EE should be present in sub-leading corrections to the area law.

Beyond the area law, many of the general results for the scaling of the EE in higher-dimensional CFTs are known primarily from the holographic EE of Ryu and Takayanagi.^{12,13} In higher-dimensional theories the geometry of the entangling regions (and the topology of space) plays a richer role. In 3+1 dimensions this richer structure allows for universal subleading logarithmic terms in the EE, even for smooth surfaces.^{13–15} Such terms are present if the entangling regions are spheres,^{16,17} and have an universal coefficient related to the two central charges of the trace anomaly of the energy-momentum tensor.⁶

In this paper we will consider the finite universal terms in the scaling of the EE both in 2+1 and 3+1 dimensions, where not many results are available. In particular, we will study the variation of this finite universal term under the twist boundary conditions. From general arguments for local field theories, relativistic or not, we know that the leading term obeys the area law. In 2+1 dimensions, for an entangling region with a smooth boundary, one expects on dimensional grounds that the subleading term should be a finite scale-invariant function of the aspect ratio(s) of the entangling region. The first example of this behavior was found in topological phases of matter in 2+1 dimensions, which are states with large-scale entanglement. In topological phases, and in topological quantum field theories such as Chern-Simons gauge theory,¹⁸ the finite term of the von Neumann EE is a constant which is given in terms of topological invariants of the underlying topological field theory and on the topology of the observed region.^{19–21}

For a 2+1-dimensional scale-invariant system, the EE of a region in the ground state satisfies the area law with a finite subleading correction, which, in general, depends on the shape of the region. This problem has been investigated in several field theories. One such theory is the quantum Lifshitz model,²² which is a free compactified scalar field in 2+1 dimensions with dynamic critical exponent $z = 2$ that describes the quantum (multi) critical

point of generalized quantum dimer models in two dimensions.^{23–26} In this model the von Neumann EE has a finite universal subleading term which depends on the compactification radius of the scalar field and of the aspect ratio (and the geometry) of the entangling surface.^{27–34} A logarithmic dependence on the size of the region was found for entangling surfaces with corners (or cusps).^{27,35}

For relativistic CFTs in 2+1 dimensions, this scaling of the EE has been shown to hold within the ϵ -expansion for an $O(N)$ scalar field at the Wilson-Fisher fixed point for a partition of the $(3 - \epsilon)$ -dimensional space into two half-spaces with a planar entangling surface.³⁶ In the limit $N \rightarrow \infty$, the von Neumann EE was recently obtained for general entangling regions.³⁷ Moreover, for a circular entangling surface, the universal subleading term of the von Neumann EE for a disk, which in this context is usually called $-F$, is a universal constant which behaves much like the central charge in 1+1-dimensional CFT in that there is an appropriately defined function $\mathcal{F}(R)$ which is monotonically decreasing along a renormalization group flow from the UV to the IR and agrees with the constant value of $F_{\text{UV,IR}}$ at the respective fixed points. This result is known as the F -theorem.^{38,39} In its strong form it was postulated within the AdS/CFT correspondence.⁴⁰ The weaker version $F_{\text{UV}} > F_{\text{IR}}$ has been first proposed in a holographic context⁴¹ and subsequently verified to hold within supersymmetric models⁴² and various other non-supersymmetric models.^{43–45} In contrast to the case of smooth boundaries, for entangling regions with corners, a logarithmic dependence in the size of the region is found also in explicit computations in relativistic models in 2+1 dimensions such as the $O(2)$ and $O(3)$ scalars at their Wilson-Fisher fixed points,^{46,47} the free massless scalar and the free massless Dirac fields,^{48,49} and by the AdS/CFT correspondence.⁵⁰ A general argument was given for the coefficient of this log for opening angles close to π in any relativistic CFT.^{51–53}

Here we will consider the ground state of scale-invariant theories in 2+1 and 3+1 dimensions on a torus and investigate the scaling of entanglement when the torus is partitioned into two cylinders. In 2+1 dimensions, the torus has circumferences L_x and L_y and the observed cylindrical region A has length L_A , as shown in Fig.1. The Rényi EE for the cylindrical region A , of aspect ratio $u = L_A/L_x$, satisfies the area law with a finite subleading correction,^{28,33,54–57}

$$S_n = \alpha \frac{2L_y}{\epsilon} - J_n(u; b) + \dots \quad (1.1)$$

where n is the Rényi index, and $b = L_x/L_y$. The leading area law term arises from short-range entanglement localized to the boundary between A and B , and is proportional to the length of the boundary, $2L_y$. The coefficient α is non-universal, being cutoff dependent. We will discuss the behavior of the finite universal term $J_n(u; b)$ in several theories on a torus with *twisted* boundary conditions, which is allowed by the non-trivial topology.

We emphasize that $J_n(u; b)$ is a *universal* scaling function that depends on the two aspect ratios: $b = L_x/L_y$ and $u = L_A/L_x$, and varies from theory to theory. It thus acts as a non-trivial fingerprint for quantum systems. It has been studied in several model systems and there are at least three analytical expressions for it. One expression was derived in the quantum Lifshitz model describing a compact free boson with dynamics exponent $z = 2$.^{30,32,33} The ground state of this model has the conformal invariance in spatial direction and therefore $J_n(u, b)$ can be analytically constructed in terms of partition functions for two-dimensional CFTs. An explicit expression on the torus has been given for $n \geq 2$.³³ The other expression was derived holographically using the Ryu-Takayanagi formula, valid within the AdS/CFT correspondence, and is expected to yield the EE for certain strongly interacting CFTs.^{12,13,55} The third instance,⁵⁶ which is the simplest, is obtained within a toy theory called the Extensive Mutual Information model.^{58,59} Although these three expressions are different, they share similar properties and take the same scaling form in various limits. The J -function can also be computed numerically for some simple theories.^{37,55–57} The $n = 2$ scaling function has also been determined by quantum Monte Carlo simulations at the quantum critical point of the two-dimensional Ising model in a transverse field by Inglis and Melko.⁵⁴ Although the quantum critical behavior of this model is described by the relativistic real scalar field at the Wilson-Fisher fixed point, Inglis and Melko found that the finite term of the second Rényi entropy is (surprisingly) well approximated by the scaling function of the quantum Lifshitz model, derived by Stephan and coworkers.³³

In this paper we study both analytically and numerically the behavior of the scaling function $J(u; b)$ for two massless relativistic models in 2+1 dimensions, the relativistic massless scalar field (which we refer to as the “free boson model”) and the massless Dirac field. We also study a free massless boson model with dynamical exponent $z = 2$ and a free fermion massless model with dynamical exponent $z = 2$ (the quadratic band touching model⁶⁰), both also in 2+1 dimensions. Although all four models are massless, and hence define scale invariant systems in 2+1 dimensions, they describe very different types of fixed points. In-

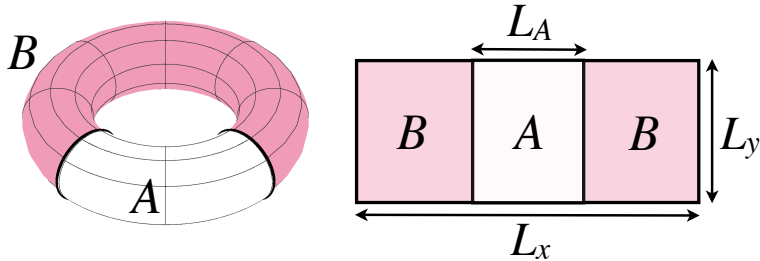


FIG. 1. The torus is divided into two cylinders A and B of size $L_A \times L_y$ and $(L_x - L_A) \times L_y$. The aspect ratios $u = L_A/L_x$ and $b = L_x/L_y$ characterize the geometry.

deed, in 2+1 dimensions the free relativistic massless scalar field is unstable in the IR, and under a $\lambda\phi^4$ perturbation flows to the Wilson-Fisher fixed point. Similarly, the free massless Dirac field is an IR stable fixed point and, as such, it defines a stable phase of matter. In contrast, both $z = 2$ theories, the free boson and the quadratic band touching fermion model describe systems at marginality (are “asymptotically free”, and hence perturbatively renormalizable). These differences make the comparisons of the scaling functions interesting. In particular, here we focus on the toroidal geometry with twisted boundary conditions, and investigate the IR flows of the EE in these geometries and compare its behavior in the free (non-compact) complex scalar field and the free (also non-compact) Dirac fermion.

We will not discuss here the interesting case of the compact relativistic boson (which should be regarded as a Goldstone boson of a spontaneously broken $U(1)$ symmetry and, hence, describes a theory at the IR stable fixed point). The entanglement properties of this model have been discussed in the literature analytically only for the geometries of disks^{61,62} and numerically on cylinders.⁶³ Likewise, we will not discuss the von Neumann EE for the compactified quantum Lifshitz model on a torus. While its entanglement properties have been extensively discussed in several geometries, for the torus the only analytical results available are for Rényi entropies with $n \geq 2$ and not the von Neumann case, $n = 1$.³³

A. Summary of the main results

In this paper, we study the function $J_n(u; b)$ in several free field theories. For the free relativistic boson CFT and the Dirac fermion CFT in 2+1 dimensions, although the complete analytical form for $J_n(u; b)$ is unknown, at around $u = 1/2$, J_n can still be analytically

obtained in the thin torus limit.³⁶ As b increases, $J_n(1/2)$ converges to a constant which only depends on the boundary condition in y direction. Here $J_n(1/2)$ is the shorthand notation for $J_n(1/2; b \rightarrow \infty)$. We also extend this calculation to $3 + 1$ dimensions and calculate $J_n(1/2)$ in the thin torus limit for various boundary conditions. We verify our analytical expression by performing numerical calculation on lattice models.

We further explore the monotonicity of $J_n(1/2)$ and the connection with the F -theorem, which states that for the $2 + 1$ dimensional relativistic CFT, the subleading correction term of the von Neumann EE for a disk is a universal constant and can serve as an RG monotone.^{17,39,42,45} We explicitly add a mass term in these free systems and define some renormalized EE so that it is equal to $J(1/2)$ when mass is zero and approaches to zero as mass increases. However, no matter how we define renormalized EE, it cannot be an RG monotone. This is because as we change the boundary condition, $J_n(1/2)$ can take both positive and negative values. A similar issue happens in $3 + 1$ dimensions, where $J_n(1/2)$ changes sign as we change the boundary condition.

We also study the $z = 2$ free boson model in $2 + 1$ dimensions with twisted boundary conditions. Since the ground state wave function has conformal invariance, we can obtain the complete $J(u, b)$ by applying the replica trick method directly on the ground state wave function. In the wide torus limit $b \rightarrow 0$, $J_n(u)$ can be exactly mapped to the corner correction $J(\theta)$ defined on an infinite plane. In the thin torus limit, $J_n(1/2)$ takes the same form as that for free boson CFT and Dirac fermion CFT up to a prefactor. For completeness, we also study the fermionic quadratic band touching model,⁶⁰ a critical fermionic system with $z = 2$, and analyze $J_n(u)$ function numerically in various limits. The main difference from the other three models in $2 + 1$ d is that $J_n(1/2)$ always equal to zero for any b .

For these $2+1$ dimensional non-interacting scale-invariant models, $J_n(u)$ in the thin torus limit $L_y \rightarrow 0$ reads

$$2\gamma_n = \begin{cases} \frac{1}{3}(1 + \frac{1}{n}) \log(2 \sin(\pi\lambda)), & \text{free complex boson CFT} \\ \frac{1}{6}(1 + \frac{1}{n}) \log(2 \sin(\pi\lambda)), & \text{Dirac fermion CFT} \\ 2 \log(2 \sin(\pi\lambda)), & z = 2 \text{ complex boson} \\ 0, & \text{fermionic quadratic band touching} \end{cases} \quad (1.2)$$

where $\lambda \in (0, 1)$ denotes the twist along the y direction and in the bosonic models, it is

defined as follows

$$\phi(x, y + L_y) = e^{i2\pi\lambda} \phi(x, y) \quad (1.3)$$

In the fermionic models, λ can be defined in the same way. $\lambda = 1/2$ corresponds to anti-periodicity. Here, γ_n is (minus) the universal EE of a semi-infinite cylindrical region obtained by bi-partitioning an infinite cylinder. For the first three theories, γ_n has the same dependence on the twist λ up to a prefactor and will diverge in the limit $\lambda \rightarrow 0$. Interestingly, the *complex* boson value of γ_n is twice that of the Dirac fermion, and the quadratic band touching has a vanishing universal contribution in this limit. We note in passing that in all four theories, γ_n vanishes identically for the special twist parameter $\lambda = 1/6$.

For the 3 + 1 dimensional complex scalar CFT, in the thin torus limit with $L_y, L_z \rightarrow 0$,

$$2\gamma_n^{3d} = \frac{1}{6} \left(1 + \frac{1}{n}\right) \log \left(\frac{\theta \left[\begin{smallmatrix} \lambda_2 - \frac{1}{2} \\ \lambda_1 - \frac{1}{2} \end{smallmatrix} \right] (\tau)}{\eta(\tau)} \frac{\theta \left[\begin{smallmatrix} \lambda_2 - \frac{1}{2} \\ -\lambda_1 + \frac{1}{2} \end{smallmatrix} \right] (\tau)}{\eta(\tau)} \right) \quad (1.4)$$

where $\tau = ir = iL_y/L_z$ is the modular parameter of each of the two boundaries of A , which are 2-tori. $\theta \left[\begin{smallmatrix} \alpha \\ \beta \end{smallmatrix} \right] (\tau)$ is given in terms of a Jacobi theta function, Eq. (B16).

The structure of this paper is as follows. We first discuss the two cylinder EE for relativistic free field theory with twisted boundary condition in 2 + 1 dimensions in Sec. III. We focus on the thin torus limit and define the renormalized EE. Then we compute two-cylinder EE defined on cylinder and torus for $z = 2$ free boson theory with twisted boundary condition in Sec. IV. We consider various limits in both cases and for comparison, we also numerically study the fermionic quadratic band touching model. We further study the two-cylinder EE for relativistic free field theory with twisted boundary condition in 3 + 1 dimensions in Sec. V. We summarize and conclude in Sec. VI. The appendices are devoted to details of the calculations and techniques used in this paper.

II. GENERAL PROPERTIES OF TORUS ENTANGLEMENT IN TWO DIMENSIONS

We review the basic properties of the universal torus function $J_n(u; b)$. Our present discussion is concerned with the thermodynamic limit of J_n , where lattice effects have been extrapolated away. First, the Rényi entanglement entropies of the cylindrical regions A and

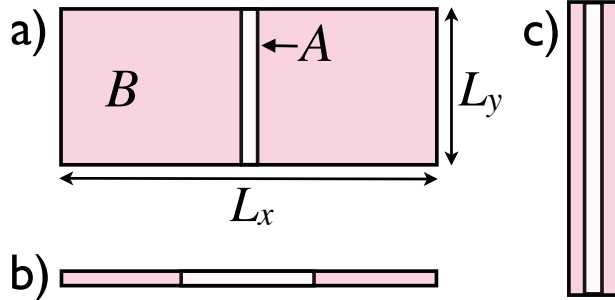


FIG. 2. Sketch of various limits of the entangling geometry on the two-dimensional torus: a) thin slice ($L_A \rightarrow 0$), b) thin torus ($L_y \rightarrow 0$) and c) wide torus ($L_y \rightarrow \infty$). In taking these limits, the other lengths are fixed. This means that a) $u \rightarrow 0$ and b finite, b) u finite and $b \rightarrow \infty$, c) u finite and $b \rightarrow 0$.

B are equal, since we work with the ground state, which is pure. This leads to the reflection symmetry: $J_n(1-u) = J_n(u)$. Further, the strong subadditive property of the EE implies⁵⁶ that $J_1(u)$ is a decreasing convex function of u on the interval $(0, 1/2]$, for any value of b and any choice of boundary conditions. For a fixed aspect ratio b , $J_1(1/2)$ is thus the smallest value of $J_1(u)$. These properties can be clearly seen in Figs. 4 and 5. We now consider various limits where we can make exact statements.

1. Thin slice limit

An important limit is the so-called thin slice limit $u \rightarrow 0$, Fig. 2 (a), where the universal term diverges as

$$J_n(u \rightarrow 0; b) = \frac{\kappa_n}{u}, \quad (2.1)$$

where κ_n is a universal coefficient characterizing the theory. Interestingly, this is the same coefficient that dictates the universal Rényi entropy of long strip living in the infinite plane: $S_{\text{strip}} = BL/\delta - \kappa L/w$, where w is the strip's width and L is a scale used to regulate the large-distance divergence. Alternatively, one can consider the EE per unit length S_{strip}/L . The reason for the appearance of the same κ in both geometries is that the boundary conditions along the x and y cycles of the torus will not influence the universal EE as $u \rightarrow 0$. (We assume, as is generically the case, that there are no zero modes in the compactified geometry.)

2. Thin torus limit

As the name suggests, we take $L_y \rightarrow 0$, while keeping L_A, L_x fixed, Fig.2 (b) . This implies that the aspect ratio diverges $b \rightarrow \infty$, while $0 < u < 1$ remains fixed. In this case, the universal Rényi entropy will tend to a constant,

$$J_n(u; b \rightarrow \infty) = 2\gamma_n, \quad (2.2)$$

where γ_n is independent of all length scales. This saturation comes about because we consider generic theories/boundary conditions precluding zero modes, so that the theory on the torus possesses a large gap $\sim 1/L_y$, and thus becomes insensitive to the length scales $L_x, L_A \gg L_y$. Further, the universal part of the EE cannot depend on L_y because no other length scale remains to form a dimensionless ratio (we work with the groundstate of a scale invariant system). In contrast, when zero modes are present (non generic), γ_n will depend on the scales L_x, L_A and the short-distance cutoff ϵ , as we illustrate in Sections III and V with the free boson and fermion with periodic boundary conditions.

3. Wide torus limit

We take the opposite limit, $b \rightarrow 0$, by sending L_y to infinity, but again keeping L_A, L_x fixed, Fig.2 (c). In this case, the EE will be dominated by the diverging length scale L_y . By translation invariance along the y -direction, J_n is expected to scale extensively with L_y :

$$J_n(u; b \rightarrow 0) = L_y \cdot \frac{f_n(u)}{L_x} = \frac{1}{b} \cdot f_n(u) \quad (2.3)$$

where we have made $f_n(u)$, which is independent of b , dimensionless by factorizing $1/L_x$. The growth of $|J_n|$ with decreasing b can be observed in Figs. 4 and 6 for the free boson and Dirac fermion CFTs, respectively. Further, in a holographic calculation⁵⁵ for an interacting CFT, it was found that the relation $J_1 = f_1(u)/b$ is exactly obeyed *for all* $b < 1$.

The J -function can be generalized to 3 + 1 dimensional theories defined on a three-torus, as shown in Fig.3.⁵⁶ In this case, J_n depends on the aspect ratio of the subsystem A , $u = L_A/L_x$, as well as on the two aspect ratios of the torus: $b_1 = L_x/L_y$ and $b_2 = L_x/L_z$. In the thin slice limit $u \rightarrow 0$, $J_n(u) \rightarrow 1/(u^2 b_1 b_2)$,⁵⁶ while in the thin torus limit $b_1, b_2 \rightarrow \infty$, J_n will saturate to $\gamma_n^{3d}(L_y/L_z)$, which only depends on the aspect ratio of the boundary of region A .

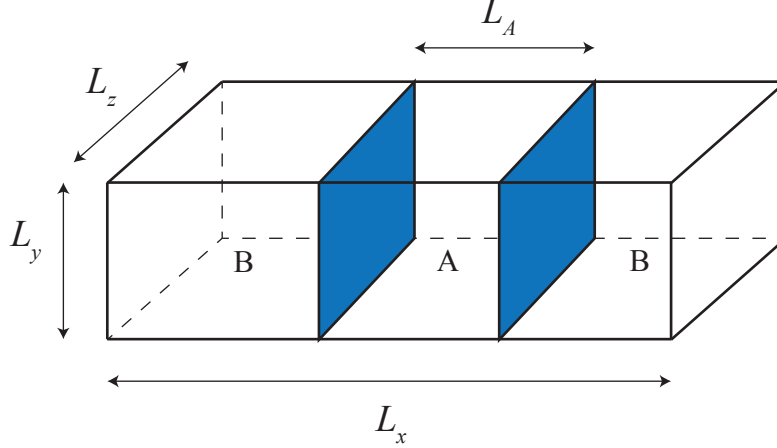


FIG. 3. Three dimensional torus, with opposite faces of the box being identified. Region A is a cylinder of length L_A , with 2 boundaries (blue/shaded).

III. TWO-CYLINDER ENTROPY FOR RELATIVISTIC FREE FIELD THEORY

The continuum Hamiltonian for the relativistic boson in 2 + 1d is

$$H = \frac{1}{2} \int dx dy (\Pi(x, y)^2 + (\nabla \phi(x, y))^2 + m^2 \phi(x, y)^2), \quad (3.1)$$

where the integral is over the $L_x \times L_y$ torus. Since the y direction is compactified into a circle of length L_y , we can decompose $\phi(x, y)$ into discrete Fourier modes in the y direction

$$\phi(x, y) = \sum_{k_y} \frac{e^{-ik_y y}}{\sqrt{L_y}} \phi_{k_y}(x) \quad (3.2)$$

with quantized momentum k_y :

$$k_y = \frac{2\pi(p + \lambda)}{L_y}, \quad (3.3)$$

where $p \in \mathbb{Z}$ and λ parametrizes the twist along the y direction. In other words, we have

$$\phi(x, y + L_y) = e^{i2\pi\lambda} \phi(x, y) \quad (3.4)$$

The twist in the x -direction is λ_x . For a real scalar field, $\phi(x, y)$ is a Hermitian operator, so λ, λ_x can only take the values 0 or 1/2, which correspond to periodic and anti-periodic boundary conditions, respectively. For a real bosonic field, the Fourier modes need to satisfy $\phi_{k_y}^\dagger(x) = \phi_{-k_y}(x)$, therefore Eq.(3.1) can be rewritten as

$$H = \sum_{k_y=-\infty}^{\infty} \frac{1}{2} \int dx \left[\Pi_{k_y}^\dagger(x) \Pi_{k_y}(x) + (\partial_x \phi_{k_y}^\dagger(x)) (\partial_x \phi_{k_y}(x)) + (m^2 + k_y^2) \phi_{k_y}^\dagger(x) \phi_{k_y}(x) \right] \quad (3.5)$$

Notice that only the $k_y \geq 0$ modes are independent degrees of freedom.

$\phi_{k_y}(x)$ can be further decomposed as follows:

$$\phi_{k_y}(x) = \frac{1}{\sqrt{2}}(\phi_{k_y,1} + i\phi_{k_y,2}) \quad (3.6)$$

The Hamiltonian becomes

$$\begin{aligned} H &= \sum_{k_y=-\infty, I=1,2}^{\infty} \frac{1}{4} \int dx \left[\Pi_{k_y,I}^2(x) + (\partial_x \phi_{k_y,I})^2 + (m^2 + k_y^2)(\phi_{k_y,I})^2 \right] \\ &= \sum_{k_y \geq 0} \frac{1}{2} \int dx \left[\Pi_{k_y,1}^2(x) + (\partial_x \phi_{k_y,1})^2 + (m^2 + k_y^2)(\phi_{k_y,1})^2 \right] \\ &\quad + \sum_{k_y > 0} \frac{1}{2} \int dx \left[\Pi_{k_y,2}^2(x) + (\partial_x \phi_{k_y,2})^2 + (m^2 + k_y^2)(\phi_{k_y,2})^2 \right] \end{aligned} \quad (3.7)$$

where we use $\phi_{k_y,I} = \phi_{-k_y,I}$ ($I = 1, 2$), and the component $\phi_{0,2} = 0$. Note that the $k_y = 0$ mode exists only when $\lambda = 0$. This Hamiltonian consists of a sum of decoupled 1 + 1d free bosons, with effective mass $\sqrt{m^2 + k_y^2}$.

Similarly, for Dirac fermions in 2 + 1d, the Hamiltonian on the torus can be expressed as a sum over an infinite number of 1 + 1-dimensional massive Dirac fermions with a mass given by $\sqrt{m^2 + k_y^2}$.

A. The shape dependence

We bi-partition the torus into two cylinders as shown in Fig. 1 and calculate the entanglement entropy between two cylinders. Since a full analytical treatment of the shape dependence for the torus EE of relativistic bosons and Dirac fermion is difficult, we compute the EE numerically by using the method explained in Appendix D. By exploiting the decomposition into decoupled (1+1)-dimensional massive chains described above, we are able to work with very large lattices. A similar analysis was previously done for the free Dirac fermion and free boson CFT, but only the quantity $-S(u) + S(1/2) = J(u) - J(1/2)$ was obtained, and only for a limited set of boundary conditions.^{55–57} Here, we determine the full $J(u; b)$, including the $J(1/2; b)$ part, by subtracting the area law contribution from S . The result is shown in Figs. 4 and 5 for the boson and fermion, respectively. In those figures, two sets of boundary conditions are used: $(\lambda_x, \lambda) = (0, 1/2)$ and $(1/2, 1/2)$, where 0 means periodic while 1/2 is anti-periodic. As mentioned in the introduction, $J_1(u)$ is a decreasing

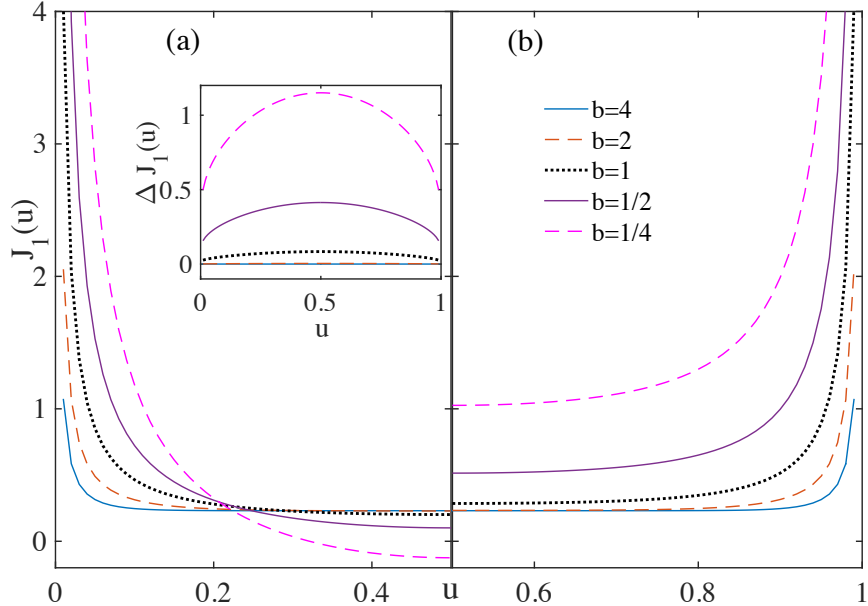


FIG. 4. (Color online) (a) The universal EE on the torus $J_1(u)$ for the non-interacting real boson CFT for various $b = L_x/L_y$ with anti-periodic boundary conditions (BCs) in the y direction and periodic BCs in the x direction: $(\lambda_x, \lambda) = (0, 1/2)$. The result is doubled for a complex boson. We use $L_x = 400$ lattice sites in the x -direction. (b) $J_1(u)$ with anti-periodic BCs in both directions: $\lambda_x = \lambda = 1/2$. The other parameters are the same as in (a). Since $J_1(u)$ is symmetric around $u = 1/2$, we only show $u \in (0, 1/2]$ in (a) and $u \in [1/2, 1)$ in (b). The inset shows the difference, $\Delta J_1(u)$, between the two choices of BCs.

convex function of u on the interval $(0, 1/2]$, for any value of b and any choice of boundary conditions. This follows from the strong subadditivity property of the EE. For a fixed aspect ratio b , the minimum of value of $J_1(u)$ is thus $J_1(1/2)$. $J_n(1/2; b)$ is plotted as function of b in Fig. 6 for both the fermion and boson, and Rényi indices $n = 1, 2$.

An important limit is the so-called thin slice limit $u \rightarrow 0$, where the universal term diverges as

$$J_n(u \rightarrow 0; b) = \frac{\kappa_n}{u} \quad (3.8)$$

where κ_n is a universal coefficient characterizing the theory. Interestingly, this is the same coefficient that dictates the universal Rényi entropy of the long thin strip. The point is that the boundary conditions along the x and y directions will not alter the value of κ (we assume

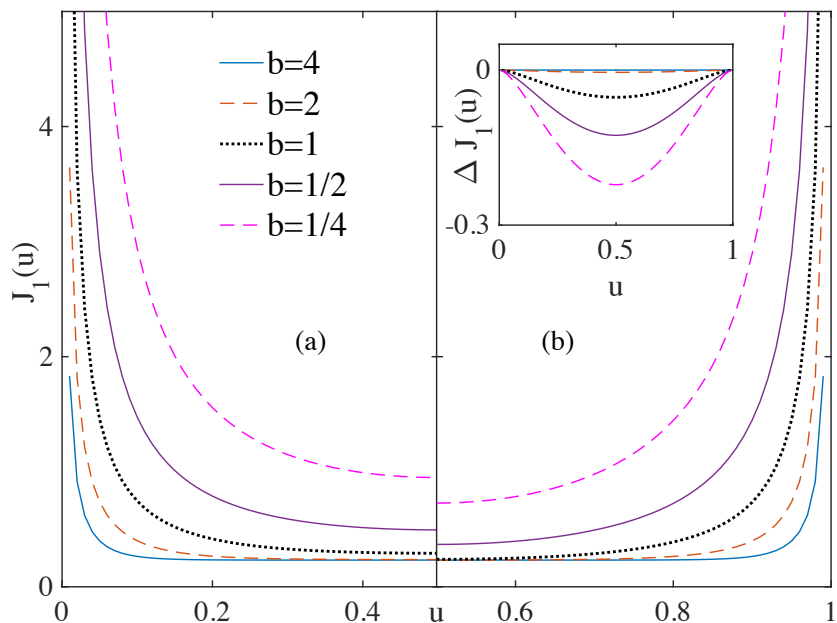


FIG. 5. (Color online) The subleading correction $J_1(u)$ of Dirac fermion for various $b = L_x/L_y$ with anti-periodic boundary condition in the y direction and periodic boundary condition in the x direction, $(\lambda_x, \lambda) = (0, 1/2)$. $L_x = 400$. (b) $J_1(u)$ with anti-periodic boundary conditions in both directions: $\lambda_x = \lambda = 1/2$. The other parameters are the same as (a). The inset shows their difference $\Delta J_1(u)$ at various b .

that both boundary conditions are not simultaneously periodic to avoid the zero mode).

B. Thin torus limit & semi-infinite cylinder

We examine another important limit, the thin torus, obtained by sending $b \rightarrow \infty$, while the ratio u remains fixed. In this case, the universal Rényi entropy saturates to a pure constant when $0 < \lambda < 1$,

$$J_n(u; b \rightarrow \infty) \rightarrow 2\gamma_n(\lambda), \quad (3.9)$$

where γ_n is the subleading term in the EE for the bi-partition of an infinite cylinder into semi-infinite cylinders, as explained in the introduction. We note that the universal constant γ_n only depends on the twist along the y -direction, λ . This becomes manifest in Figs. 4-5, where the left panels have $\lambda_x = 0$, while the right ones have $\lambda_x = 1/2$. Their differences,

$\Delta J_1(u)$, for the two choices of x -boundary conditions are shown in the insets. Indeed, at large b , $J_1(u)$ becomes insensitive to λ_x , and $\Delta J_1(u) \approx 0$.

We can analytically compute γ_n for all n using the 1d decomposition given above, Eq.(3.7). For a finite interval of length L_A , each 1 + 1d massive chain, with effective mass $\sqrt{m^2 + k_y^2}$, contributes an EE³

$$S_n^{\text{1d}}(k_y) = -\frac{1}{12} \left(1 + \frac{1}{n}\right) \log [(m^2 + k_y^2)\epsilon^2] \quad (3.10)$$

where the length of the interval is taken to be much larger than the inverse mass, $L_A \gg 1/\sqrt{m^2 + k_y^2}$; ϵ is the UV cutoff, and n the Rényi index. The total EE is then

$$S_n = -\sum_{k_y} \frac{1}{12} \left(1 + \frac{1}{n}\right) \log [(m^2 + k_y^2)\epsilon^2] \quad (3.11)$$

We first consider the massless case, $m = 0$,

$$S_n = -\sum_{p \in \mathbb{Z}} \frac{1}{6} \left(1 + \frac{1}{n}\right) \left(\log |2\pi(p + \lambda)| + \log \frac{\epsilon}{L_y} \right) \quad (3.12)$$

where $k_y = 2\pi(p + \lambda)/L_y$. λ denotes the twist boundary condition in the y direction, $\phi(x, y + L_y) = e^{2\pi i \lambda} \phi(x, y)$. This expression can be regularized and we get

$$S_n = \alpha \frac{L_y}{\epsilon} - 2\gamma_n \quad (3.13)$$

By using the Hurwitz zeta function regularization method discussed in Appendix B 1, we have for $0 < \lambda < 1$

$$2\gamma_n = \sum_{p \in \mathbb{Z}} \frac{1}{6} \left(1 + \frac{1}{n}\right) \log |p + \lambda| = \frac{1}{6} \left(1 + \frac{1}{n}\right) \log(2 \sin(\pi \lambda)) \quad (3.14)$$

For the real boson field, λ can only be 0 or 1/2. When $\lambda = 1/2$, $2\gamma_1 = \frac{\log 2}{3} = 0.231$. This matches the numerical results shown in Fig. 6. For the Dirac fermion, λ can take values between 0 and 1, which corresponds to arbitrary twisted boundary condition and can be realized by coupling Dirac fermion to a $U(1)$ gauge field. In this case, γ_n takes the same formula shown in Eq.(3.14). For a *complex* boson, $\lambda \in (0, 1)$ and γ_n is twice of that for real boson field or Dirac fermion field. γ_n in the thin torus limit takes the same form for both $z = 1$ free boson and Dirac fermion model.

Strictly speaking, Eq.(3.14) only works for $0 < \lambda < 1$. As $\lambda \rightarrow 0$, the effective mass of the $k_y = 0$ (1 + 1)d mode vanishes and the use of Eq.(3.14) will yield an incorrect result.

This issue can be resolved by separately treating the massive modes $k_y \neq 0$ and the zero mode with $k_y = 0$. The $k_y = 0$ zero mode contributes a subleading term to the EE that will depend on the aspect ratio $u = L_A/L_x$, as well as on L_x/ϵ , where ϵ is the UV cutoff. In addition, this subleading term *will depend on the twist along the x -direction*, λ_x . Since the zero mode is not suppressed by a $\sim 1/L_y$ gap, it is sensitive to the entire geometry, including the boundary conditions along the “long direction”, x . For the special case of periodic boundary conditions along x , $\lambda_x = 0$, we obtain

$$2\gamma_n = -\frac{1}{6} \left(1 + \frac{1}{n}\right) \log \left(\frac{L_x}{\pi\epsilon} \sin \left(\frac{\pi L_A}{L_x} \right) \right) \quad (3.15)$$

The massive modes, after regularization, contribute a finite non-universal constant.

Eq.(3.15) shows a $\log(1/\epsilon)$ divergence, is the classic “chord-length” expression for the EE of a single interval in a 1+1d CFT on a circle³. The scaling in Eq.(3.15) was numerically observed for a massless Dirac fermion on a thin torus in Ref. 55. We note that when a small twist along y is introduced, $\lambda > 0$, it induces an order λ mass for the zero mode that cuts off the $\log(L_A/\epsilon)$ divergence to $\log(1/\lambda)$.

At $\lambda = 0$ but for generic λ_x , the answer for γ_n is expected to differ from Eq.(3.15). Indeed, in the case of a real (1+1)d boson with anti-periodic boundary conditions $\lambda_x = 1/2$, numerical calculations on the lattice⁵⁷ have shown deviations from Eq.(3.15). More recently, the Rényi entropies for a free boson CFT with Rényi index $n \neq 1$ were analytically computed as a function of λ_x by Shiba⁶⁴, and they differ from Eq.(3.15). See the Added Note after the Conclusions.

Finally, before moving to the massive case, we want to emphasize a subtle difference between our analytical and numerical calculation. For the free boson model in Eq.(3.7), we expressed the Hamiltonian in the continuum, hence we have a sum over a set of discrete and yet infinite number of Fourier modes in Eq.(3.11). Alternatively, we can consider a lattice version of the free boson Hamiltonian defined on the torus, given in Eq.(D8). The effective mass for each 1 + 1d chain then changes to $\sqrt{2 - 2\cos(k_y) + m^2}$ (where the lattice spacing is set unity), and we only need to sum over a finite number of momenta. In the limit of large lattices that we consider, our results agree with the analytical calculations performed in the continuum. In the thin torus limit, a detailed comparison between the analytical and lattice results is presented in Fig. 6, where good agreement is found.

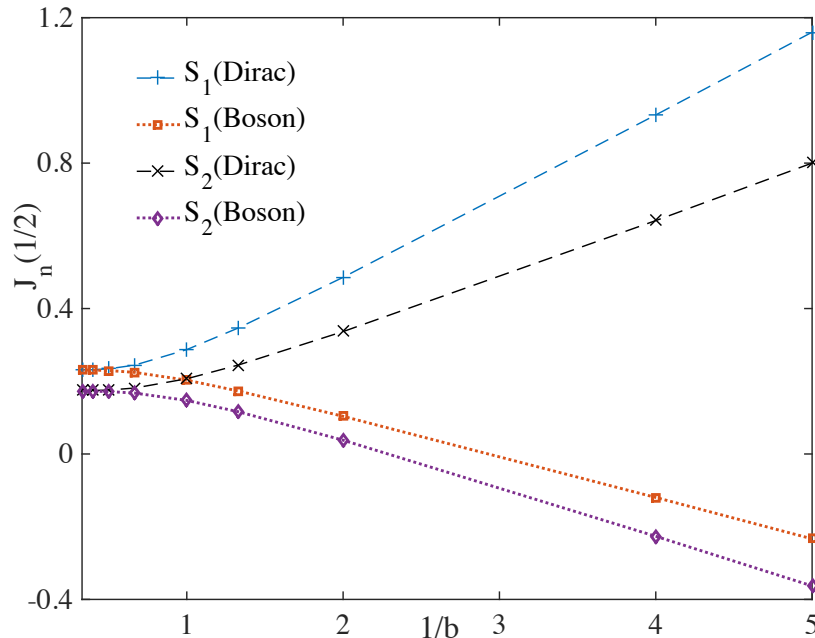


FIG. 6. (Color online) Numerical lattice calculation of $J_n(1/2; b)$ as a function of $1/b$ for a real boson and a 2-component Dirac fermion. We choose anti-periodic boundary conditions along y , and periodic boundary condition along x . When $n = 1$, $J_1(1/2; b \gg 1)$ converges to 0.2310 and when $n = 2$, $J_2(1/2; b \gg 1)$ converges to 0.174. Every data point is obtained by increasing L_y from 400 to 720 and subtracting the leading area law term.

1. Massive case

We now consider the effect of adding a mass to the theory, leading to a $m^2\phi^2$ term in the Lagrangian. We note that for periodic boundary conditions ($\lambda = 0$), a finite mass needs to be introduced to cure the divergence of γ_n , Eq.(3.14). Therefore we need to calculate this infinite sum

$$g(\lambda, mL_y) = \sum_{p=-\infty}^{\infty} \log [(mL_y)^2 + (2\pi)^2(p + \lambda)^2] \quad (3.16)$$

This can be regularized by using the Epstein zeta function regularization method (see Appendix B2), and we have

$$g(\lambda, mL_y) = \log [2 \cosh(mL_y) - 2 \cos(2\pi\lambda)] \quad (3.17)$$

This bare result was also computed in Ref. [37] and Ref. [65]. Naively, the universal EE would then be proportional to this quantity. However, we notice a strange property: Eq.(3.17)

diverges linearly in the large mass limit, $g(\lambda, mL_y \gg 1) = mL_y + \dots$. This is at odds with the intuition that the infinite mass fixed point, which describes a state without spatial entanglement, should have $\gamma = 0$. This divergence points to a deeper problem with our naive procedure to extract the universal EE by subtracting the area law contribution. Indeed, when the theory is away from the massless fixed point, the additional length scale $1/m$ renders the subtraction procedure ambiguous. A similar situation occurs when considering the EE of a region A in infinite flat space instead of a torus. For example when A is a perfect disk living in \mathbb{R}^2 , the universal subleading term in the EE is often called $-F$. A statement called the F -theorem has been shown for relativistic theories:³⁸ F decreases monotonically along an RG flow. If we thus have a UV CFT that flows into an IR one, the following inequality will hold $F_{\text{UV}} > F_{\text{IR}}$. Now, for a free massive boson, a naive computation of F by subtraction of the area law leads to linear divergence $F \sim -mR$ at large mass. Here, R is the radius of the disk. This is exactly analogous to the divergence that we have seen in Eq.(3.17). However, the divergence of F is at odds with the F -theorem since the infinite mass fixed point is trivial, and has $F = 0$. The cure for the disk is known: one needs to consider a *renormalized* EE, $\mathcal{F}(R) = -S + R \frac{\partial S}{\partial R}$, where S is the full EE (computed using any given regulator).^{38,40} At conformal fixed points, $\mathcal{F} = F$ agrees with the expected CFT value, while $\mathcal{F}(R)$ decreases monotonically along an RG flow linking two fixed points.

Going back to our situation on the torus, we can define a renormalized γ as follows:⁶⁶

$$2\tilde{\gamma}(L_y) = -S + L_y \frac{\partial S}{\partial L_y}, \quad (3.18)$$

where S is here evaluated in the thin torus limit $b \rightarrow \infty$. (This can be naturally generalized beyond the thin torus limit to all u, b .⁶⁶) Eq. (3.18) is the one-to-one analogue of the renormalized disk EE used in the F -theorem, discussed above. In contrast to the F -theorem however, there is no proof that this quantity is the “natural” one to consider, in the sense of being an RG monotone, say. Our motivation for using Eq.(3.18) for defining the EE away from a fixed point is its simplicity, and its connection to the disk EE prescription (which is also non-unique when A is not a disk). In the case of the massive complex boson, we thus find:

$$\begin{aligned} 2\tilde{\gamma}_n(mL_y) &= \frac{1}{6} \left(1 + \frac{1}{n}\right) \left[g(\lambda, mL_y) - L_y \frac{\partial g(\lambda, mL_y)}{\partial L_y} \right] \\ &= \frac{1}{6} \left(1 + \frac{1}{n}\right) \left\{ \log[2 \cosh(mL_y) - 2 \cos(2\pi\lambda)] - \frac{mL_y \sinh(mL_y)}{\cosh(mL_y) - \cos(2\pi\lambda)} \right\} \end{aligned} \quad (3.19)$$

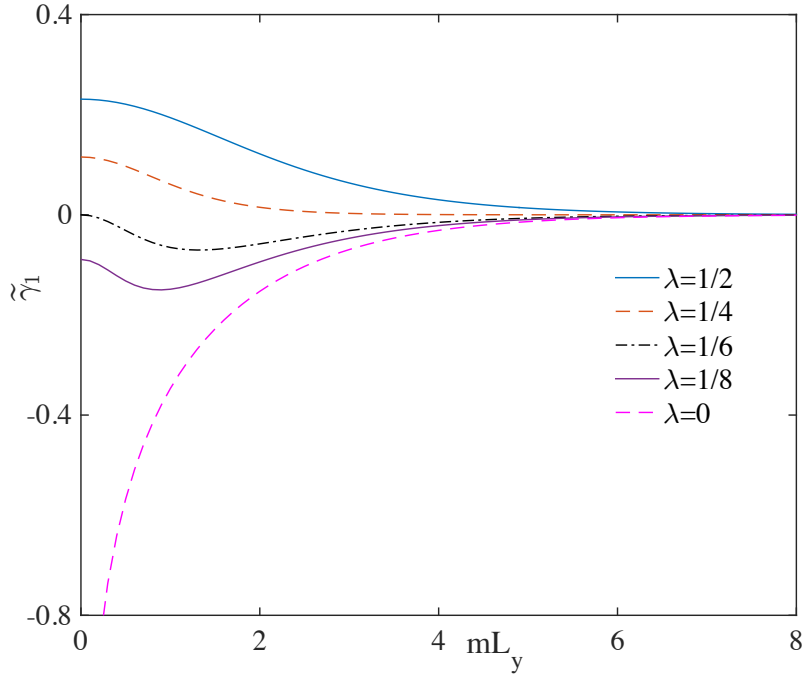


FIG. 7. (Color online) The renormalized EE $\tilde{\gamma}_1$ for the complex boson (or two Dirac fermions), Eq.(3.19), as a function of mL_y for various twists λ . For periodic boundary conditions, $\lambda=0$, there is a divergence $-\log(mL_y)$ as $mL_y \rightarrow 0$. This agrees with the fact that γ has a log dependence on the cutoff ϵ when $m = \lambda = 0$, see (3.15).

In the small and large $t = mL_y$ limits, the renormalized EE becomes

$$\tilde{\gamma}_1(t \rightarrow 0) = \gamma_1 - \frac{t^2}{48 \sin^2(\pi\lambda)} + \frac{t^4(2 + \cos(2\pi\lambda))}{384 \sin^4(\pi\lambda)} + O(t^6) \quad (3.20)$$

$$\tilde{\gamma}_1(t \rightarrow \infty) = -\frac{\cos(2\pi\lambda)}{6} t e^{-t} + \dots \quad (3.21)$$

respectively. We see that the leading correction at small t is always negative, i.e. $\tilde{\gamma}_n$ initially decreases under the RG flow, irrespective of λ . Interestingly, a similar result was found in the context of strongly interacting holographic CFTs at $n = 1$.⁶⁶ It would be interesting to investigate the RG flow of $\tilde{\gamma}$ in the vicinity of more general UV fixed points (weak detuning regime), in the same spirit as was done for the EE of a disk.⁶⁷ Second, we observe that $\tilde{\gamma}_n$ decays to zero exponentially fast in the deep IR limit $t \rightarrow \infty$, Eq.(3.21), as shown in Fig. 7. However, as shown in that figure, it is not a monotonically decreasing function for all values of the twist λ . Indeed, Eq. (3.21) shows that $\tilde{\gamma}_n$ becomes strictly increasing at large t when $0 < \lambda < 1/4$. The non-monotonicity could have been anticipated because when $m = 0$, γ_n

can be strictly negative for certain values of λ , and we know that at the trivial infinite mass fixed point it will vanish, $\tilde{\gamma}_n = 0$. Interestingly, at $\lambda = 1/6$, $\tilde{\gamma}_n$ is zero at both fixed points, $mL_y = 0$ and ∞ . However, it is a non-trivial function along the RG flow that interpolates between these two fixed points, as shown in Fig. 7.

IV. $z = 2$ FREE BOSONS & FERMIONS WITH A TWIST

In this section we study the torus EE of two non-relativistic gapless systems: the non-interacting boson with dynamical exponent $z = 2$, and the fermionic quadratic band touching (which also has $z = 2$).

A. $z = 2$ free bosons

The Hamiltonian for free boson field ϕ with dynamical scaling exponent $z = 2$ is

$$H = \int d^2x \frac{1}{2} \left(\Pi^2 + [\nabla^2 \phi]^2 \right), \quad (4.1)$$

where Π is its conjugate canonical momentum. When ϕ is compact (i.e., $\phi \equiv \phi + 2\pi R$), this model is quantum Lifshitz model and describes the quantum dimer model at critical point.²² There has been a lot of references discussing EE in this model.²⁷⁻³⁴ Here we study the entanglement of the non-compact version, focusing on the subleading universal term on the torus, when there is a twist in the y direction. The ground state wavefunction of Eq.(4.1) has a simple and elegant form

$$|\psi\rangle = \frac{1}{\sqrt{\mathcal{Z}}} \int [d\phi] e^{-\frac{1}{2}\mathcal{S}[\phi]} |\phi\rangle. \quad (4.2)$$

Here \mathcal{Z} is the partition function of the free boson CFT in a two-dimensional Euclidean spacetime, and $\mathcal{S}[\phi]$ is the corresponding Euclidean action,

$$Z = \int [d\phi] e^{-\mathcal{S}[\phi]}, \quad \mathcal{S}[\phi] = \frac{1}{2} \int d^2x (\nabla\phi)^2 \quad (4.3)$$

For the above wave function, if ϕ is non-compact, by using the replica trick directly on the wave function, we have²⁷

$$\text{Tr } \rho_A^n = \left(\frac{Z(A)Z(B)}{Z(A \cup B)} \right)^{n-1} \quad (4.4)$$

where $Z(A)$ and $Z(B)$ are the free boson partition functions on region A and B , respectively, with Dirichlet boundary condition $\phi = 0$ on the boundary. $Z(A \cup B)$ is the boson partition function on the entire space, with the same boundary conditions as those imposed on the 2+1 dimensional theory. The Rényi entanglement entropy is then

$$S_n = -\log \frac{Z(A)Z(B)}{Z(A \cup B)}, \quad (4.5)$$

which is independent of the Rényi index n . Below we consider the entire system $A \cup B$ to be an open cylinder and torus, respectively.

1. Two-cylinder entropy on a cylinder

We first study the groundstate on the open cylinder and calculate the two-cylinder EE with twisted boundary condition in the y direction, which is also denoted by λ and is defined through $\phi(x, y + L_y) = e^{2\pi i \lambda} \phi(x, y)$. We impose Dirichlet boundary condition with $\phi = 0$ on both ends of the entire cylinder $A \cup B$. As shown in Fig. 8, $Z(A)$, $Z(B)$ and $Z(A \cup B)$ are all partition functions defined on cylinder. For the real boson, the only possible twist boundary condition corresponds to $\lambda = 1/2$. Under this twist, the partition function of the cylinder (after regularization) is equal to

$$Z = \sqrt{2} \sqrt{\frac{\eta(-\frac{1}{2\tau})}{\theta_2(-\frac{1}{2\tau})}} = \sqrt{2} \sqrt{\frac{\eta(2\tau)}{\theta_4(2\tau)}} \quad (4.6)$$

where $\tau = iL_x/L_y$ is the modular parameter and $u = L_A/L_x$. The explicit form of $\eta(\tau)$, $\theta_2(\tau)$ and $\theta_4(\tau)$ are shown in Appendix A. According to Eq.(4.5), the subleading correction $-\mathcal{J}_n(u)$ of EE is equal to

$$\mathcal{J}_n(u) = \frac{1}{2} \log \left(\frac{2\eta(2u\tau)\eta(2(1-u)\tau)\theta_4(2\tau)}{\eta(2\tau)\theta_4(2u\tau)\theta_4(2(1-u)\tau)} \right) \quad (4.7)$$

In the thin cylinder limit $\tau \rightarrow \infty$, if the ratio u takes a finite value, the cylinder partition function $Z \rightarrow \sqrt{2}$ and therefore $\mathcal{J}_n(u) = \log(\sqrt{2} \times \sqrt{2}/\sqrt{2}) = \log(\sqrt{2})$.

For a complex boson, $\lambda \in (0, 1)$. The partition function on the cylinder (after regulariza-

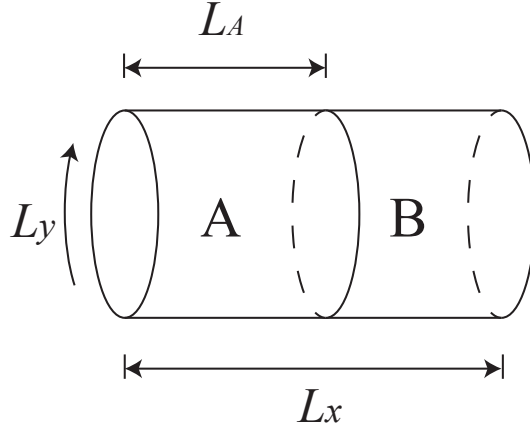


FIG. 8. Bipartition of a cylindrical geometry. We impose Dirichlet boundary conditions $\phi = 0$ at both ends. The universal part of the EE is $-\mathcal{J}$, which is generally distinct from the analogous quantity defined on a torus, $-J$.

tion) under a general twist is equal to

$$\begin{aligned}
 Z &= e^{\pi i(\lambda - \frac{1}{2})} (1 - e^{-2\pi i \lambda}) \frac{\eta(-\frac{1}{2\tau})}{\theta\left[\begin{smallmatrix} \frac{1}{2} \\ \lambda - \frac{1}{2} \end{smallmatrix}\right](-\frac{1}{2\tau})} \\
 &= (1 - e^{-2\pi i \lambda}) \frac{\eta(2\tau)}{\theta\left[\begin{smallmatrix} \lambda - \frac{1}{2} \\ -\frac{1}{2} \end{smallmatrix}\right](2\tau)}
 \end{aligned} \tag{4.8}$$

The explicit form of the $\theta\left[\begin{smallmatrix} \alpha \\ \beta \end{smallmatrix}\right](\tau)$ function is given in Eq.(A1). According to Eq.(4.5), the universal EE contribution for the two-cylinder bi-partition of the open cylinder in case of a complex boson is

$$\mathcal{J}_n(u) = \log \left(\frac{\eta(2u\tau)\eta(2(1-u)\tau)\theta\left[\begin{smallmatrix} \lambda - \frac{1}{2} \\ -\frac{1}{2} \end{smallmatrix}\right](2\tau)}{\eta(2\tau)\theta\left[\begin{smallmatrix} \lambda - \frac{1}{2} \\ -\frac{1}{2} \end{smallmatrix}\right](2u\tau)\theta\left[\begin{smallmatrix} \lambda - \frac{1}{2} \\ -\frac{1}{2} \end{smallmatrix}\right](2(1-u)\tau)} \right) + \log(1 - e^{-2\pi i \lambda}) \tag{4.9}$$

$\mathcal{J}_n(u)$ here is written in terms of theta and Dedekind η functions, and is fairly non-trivial. In the following sections, we examine various limits of \mathcal{J}_n .

a. Thin slice limit: The partition function for cylinder A of the complex boson is equal to

$$Z(A) = e^{\frac{\pi}{12ub}} \prod_{n=1}^{\infty} \frac{1}{(1 - e^{2\pi i \lambda} e^{-\frac{\pi n}{ub}})(1 - e^{-2\pi i \lambda} e^{-\frac{\pi n}{ub}})} \tag{4.10}$$

If we keep the ratio $b = L_x/L_y$ finite in the thin slice limit $u \rightarrow 0$, $Z(A) \rightarrow e^{\frac{\pi}{12ub}}$. The remaining contribution to S_n is $\log[Z(B)/Z(A \cup B)] \approx 0$, and therefore we have

$$\mathcal{J}_n(u \rightarrow 0) = \frac{\pi c}{24ub} = \frac{\pi c L_y}{24L_A} \quad (4.11)$$

where c is the central charge for the classical two dimensional conformal field theory. For the complex boson we discuss here, it is equal to $c = 2$, while for the real boson, $c = 1$. Notice that in this limit, $\mathcal{J}_n(u)$ is independent of the twists in the x and y directions.

b. Thin cylinder limit: We take $L_y \rightarrow 0$ at fixed u , which means $\tau \rightarrow i\infty$. Then the first term in Eq.(4.9) is equal to $\log(e^{\pi i(\lambda - \frac{1}{2})})$. When combined with the second term in S_n , we find that the EE saturates to a constant independent of any length scale, γ_n :

$$\gamma_n = \log \left[(1 - e^{-2\pi i \lambda}) e^{\pi i(\lambda - \frac{1}{2})} \right] = \log [2 \sin(\pi \lambda)] \quad (4.12)$$

which is exactly the same γ_n that appears in the universal EE of a thin *torus*, Eq.(1.2) and Eq.(4.15) below. However, in the torus case the EE tends to $2\gamma_n$ instead because of the presence of two boundaries. The agreement, up to this trivial factor of 2, between the open-cylinder and torus geometries in the $L_y \rightarrow 0$ limit follows because the EE is insensitive to degrees of freedom far from the entanglement cut, where distances ought to be compared to the limiting length scale L_y . We note that the λ -dependence of γ_n for the $z = 2$ boson is the same as for the $2 + 1$ dimensional free boson and Dirac fermion CFTs, as given in Eq.(3.14), up to an overall prefactor.

The \mathcal{J} -function in Eq.(4.9) can be compared with that for the quantum Lifshitz model, which takes this form on the open cylinder:³⁴

$$\mathcal{J}_1^{\text{QLM}}(u) = \log \left| \frac{\eta(2\tau)}{\eta(2\tau u)\eta(2\tau(1-u))} \right| - \frac{1}{2} \log[2u(1-u)|\tau|] + W(\tau, R) \quad (4.13)$$

where $W(\tau, R)$ is a u -independent term coming from the zero mode sector for the compact boson with compactification radius R . The boson is here assumed to be periodic along y . In the thin slice limit, $\mathcal{J}_1^{\text{QLM}}(u \rightarrow 0) = \pi/(24ub)$, which is the same as \mathcal{J}_1 of the non-compact $z = 2$ boson, Eq.(4.9). In the thin cylinder limit, $L_y \rightarrow 0$, $\mathcal{J}_1^{\text{QLM}}$ tends to a shape-independent constant, $-\log(\sqrt{4\pi}R) + \frac{1}{2}$, which only depends on R .^{28,30,31} As $R \rightarrow \infty$, one recovers the non-compact boson answer. Indeed $\mathcal{J}_1^{\text{QLM}} \rightarrow -\infty$ is the same as γ_1 in the non-compact case in the limit $\lambda \rightarrow 0$, Eq.(4.12).

2. Two-cylinder entropy on a torus

If the total system is on a torus, there are two boundaries between A and B . By using the partition function of the torus $Z(A \cup B)$, Eq.(C13), we can write down the J -function for two-cylinder EE defined on the torus,

$$J_n(u) = \log \left(\frac{\eta(2u\tau)\eta(2(1-u)\tau)\theta \left[\begin{smallmatrix} \lambda - \frac{1}{2} \\ -\lambda_x + \frac{1}{2} \end{smallmatrix} \right](\tau)\theta \left[\begin{smallmatrix} -\lambda + \frac{1}{2} \\ -\lambda_x + \frac{1}{2} \end{smallmatrix} \right](\tau)}{\eta^2(\tau)\theta \left[\begin{smallmatrix} \lambda - \frac{1}{2} \\ -\frac{1}{2} \end{smallmatrix} \right](2u\tau)\theta \left[\begin{smallmatrix} \lambda - \frac{1}{2} \\ -\frac{1}{2} \end{smallmatrix} \right](2(1-u)\tau)} \right) + 2 \log(1 - e^{-2\pi i \lambda}) \quad (4.14)$$

where λ_x and λ represent the twists in x and y directions, respectively.

a. Thin torus limit: In the thin torus limit, $J_n(u)$ approaches a constant $2\gamma_n$ when $\lambda > 0$, which is independent of λ_x , and is twice the value of the corresponding coefficient for a bipartition of an infinite cylinder into two equal halves:

$$2\gamma_n = 2 \log \left[(1 - e^{-2\pi i \lambda}) e^{\pi i (\lambda - \frac{1}{2})} \right] = 2 \log (2 \sin(\pi \lambda)). \quad (4.15)$$

The overall factor of 2 arises because of the two boundaries between A and B . Therefore, the $z = 2$ massless free boson, free boson CFT and Dirac fermion CFT all have the same twist dependence but with different overall prefactors. We numerically obtain $2\gamma_1$ by calculating $J_1(1/2)$ on the lattice at large b for these three models and the results are shown in Fig. 9. For λ close to $1/2$, the numerical results agree perfectly with the analytical expression for $2\gamma_1$. As λ decreases, the Dirac fermion and free boson CFT start to show deviations from $2\gamma_1$. This is because as λ decreases, the $1+1$ -dimensional modes around $k_y = 0$ have smaller effective masses, and larger b and L_y are therefore required to obtain better agreement.

b. Wide torus limit: We now consider the limit opposite to the thin torus one, namely the wide torus: $L_y/L_x \rightarrow \infty$ (Fig.2 (c)). If u is finite, we have

$$\log Z(A) + \log Z(B) = \frac{\pi c}{24} \frac{1}{bu(1-u)} \quad (4.16)$$

This result is obtained by using the derivation in Eq.(C19). In contrast, the partition function $Z(A \cup B)$ on the entire torus will contribute a u -independent term. In the limit $b \rightarrow 0$, it is

$$\log Z(A \cup B) = \frac{\pi c}{6b} \quad (4.17)$$

Therefore we have

$$J_n(u) = \frac{\pi c}{24b} \frac{1}{u(1-u)} - \frac{\pi c}{6b} \quad (4.18)$$

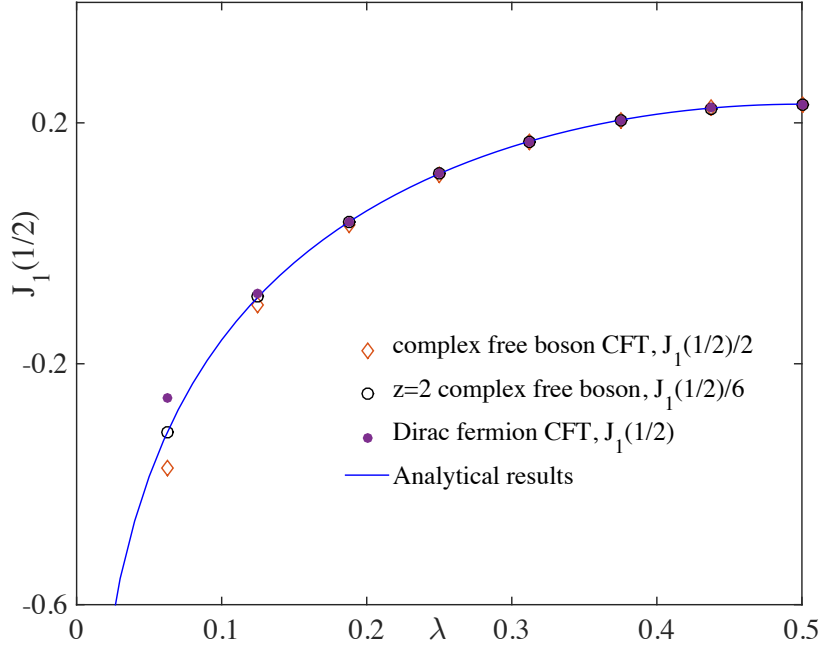


FIG. 9. (Color online) The two cylinder EE on the torus $J_1(1/2)$ at $b = 6$ versus the twist parameter along the y -direction, λ . For such a large value of b , $J_1(1/2)$ approaches $2\gamma_1$, Eq. (1.2). We have rescaled the data so that it collapses to one curve: $\frac{1}{3} \log[2 \sin(\pi\lambda)]$. For the bosonic models, each point is obtained by taking L_y from 200 to 400 and subtracting the area law term. For the Dirac fermion, each point is obtained by taking L_y from 200 to 320 and subtracting the area law term. The $z = 2$ free boson model matches best with the analytical expression. The mismatch for free boson and Dirac fermion CFTs at small λ is due to finite size effects.

where for a real bosonic field, $c = 1$, while $c = 2$ for the complex boson. Eq.(4.18) can be re-written as

$$J_n(u) = \frac{2\pi}{b} a_n(\theta), \quad \theta = 2\pi u, \quad (4.19)$$

where

$$a_n(\theta) = \frac{c}{12} \frac{(\theta - \pi)^2}{\theta(2\pi - \theta)} \quad (4.20)$$

We have used the natural mapping between the cylinder's normalized length u , and the angle $\theta = 2\pi u$. Actually, $a_n(\theta)$ is the coefficient of the logarithmic term in the EE for the $z = 2$ boson that arises in the presence of a sharp corner of opening angle θ in the entangling surface.²⁷ This is because the infinite cylinder can be mapped to the infinite plane through

a conformal transformation. The transformation maps an infinite strip of width u living on the cylinder to a wedge of angle $\theta = 2\pi u$ on the plane. To make this clear, we can also directly calculate the corner correction of EE for $z = 2$ boson model. Since $\log Z$ for a wedge with opening angle θ is equal to⁶⁸

$$\log Z = -\frac{c\theta}{24\pi} \left(1 - \frac{\pi^2}{\theta^2}\right) \log(L/\epsilon), \quad (4.21)$$

Following Ref. 27, one readily finds that the contribution to the entanglement entropies follows from adding the corner contribution to the free energies of regions A (with angle θ) and B (with angle $2\pi - \theta$), leading to the result that the Rényi entropies have a subleading logarithmic contribution associated with a corner of angle θ of the form

$$S_n = B_n L - a_n(\theta) \log(L/\epsilon) + \dots \quad (4.22)$$

where the corner coefficient for the $z = 2$ boson is given in Eq.(4.20). We emphasize that this direct relation between the wide-torus limit of $J_n(u)$ and the corner coefficient $a_n(\theta)$ arises here because the ground state is invariant under the infinite group of two-dimensional conformal transformations.²² This is not the case for general critical theories like the gapless boson and Dirac fermion CFTs.

The case $\lambda = 0$ must be treated separately, just as was done for CFTs. We leave such analysis for the future.

B. Fermionic quadratic band touching

The fermionic quadratic band touching (QBT) model describes free fermions with a quadratic energy dispersion ($z = 2$). The low-energy Hamiltonian for the QBT takes the form

$$H = \int \frac{d^2k}{(2\pi)^2} \Psi^\dagger(k) \begin{pmatrix} k_x^2 - k_y^2 & -2ik_x k_y \\ 2ik_x k_y & -k_x^2 + k_y^2 \end{pmatrix} \Psi(k), \quad (4.23)$$

where we have defined the two-component spinor $\Psi(k) = (\psi_1(k), \psi_2(k))^T$. We have set the band-curvature scale M to unity, $k_i k_j / M \rightarrow k_i k_j$, as it will play no role in our discussion. In contrast to the Dirac fermion, this model corresponds to a critical point not a critical phase, and has a finite density of states at the band touching point.⁶⁰

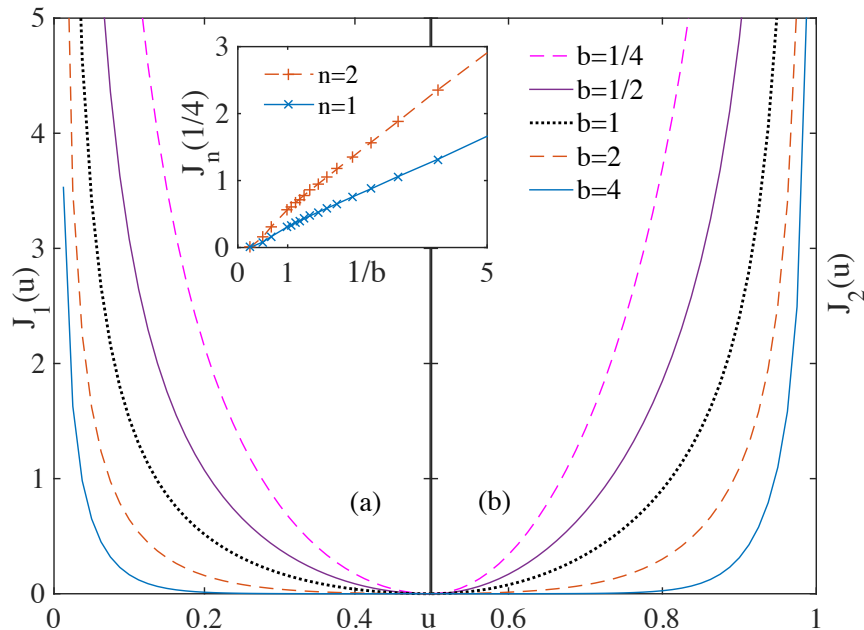


FIG. 10. (Color online) The universal contribution $J_1(u)$ of the QBT model for various aspect ratios $b = L_x/L_y$, with anti-periodic boundary condition in the y -direction and periodic boundary condition in x . $L_x = 320$. The inset shows $J_n(1/4)$ as a function of $1/b$, where the line is a guide to the eye.

The QBT model naturally satisfies the area law due to the absence of an extended Fermi surface. On the square torus, $b = 1$, the u -dependence of the correction $J_1(u) - J_1(1/2)$ has been numerically studied in Ref. 55. Unlike for the $z = 2$ free boson model, it is not known whether the groundstate for QBT model is connected to a two dimensional CFT, and therefore the analytical methods used to study the $z = 2$ free boson cannot be applied.

We numerically study the u and b dependence of $J_n(u; b)$ and find that the different Rényi indices lead to similar behavior. Therefore we will focus only on $n = 1, 2$. Different from the other three models we have studied in $2 + 1$ dimensions, we find that when A covers half the torus, $J_n(1/2; b)$ vanishes for arbitrary boundary conditions along x and y :

$$J_n(1/2; b) = 0. \quad (4.24)$$

This is true for *all* aspect ratios b . In particular, taking the thin torus limit $b \rightarrow \infty$, Eq. (4.24) implies that $\gamma_n = 0$. This behavior at $u = 1/2$ distinguishes the QBT from all

the critical theories that have been studied so far, and it would be interesting to understand the physical reasons underlying Eq. (4.24). As shown in Fig. 10, as $u \rightarrow 1/2$, all the curves indeed approach zero.

In the wide torus limit, $b \rightarrow 0$, we previously found that the $z = 2$ boson has $\lim_{b \rightarrow 0} bJ_n(1/2; b) = 0$, which also holds for the QBT by virtue of Eq. (4.24). In contrast, the non-interacting boson and Dirac fermion CFTs have $J_n(1/2) \sim 1/b$ as $b \rightarrow 0$. This is also the case for certain CFTs described by the AdS/CFT holographic correspondence.⁵⁵ For $u \neq 1/2$, when $b \ll 1$, the QBT has $J_n(u) \sim 1/b$, in accordance with our general argument. In the inset of Fig. 10, we plot $J_1(1/4)$ and $J_2(1/4)$ as a function of $1/b$ to illustrate this fact.

In the thin slice limit $u \rightarrow 0$, taken at fixed b , we obtain the expected divergence^{55,56} $J_n(u) = \kappa_n/(bu) = \kappa_n L_y/L_A$, with

$$\kappa_1 = 0.182, \quad \kappa_2 = 0.263. \quad (4.25)$$

We first note that $\kappa_2 > \kappa_1$, which is distinct from the behavior exhibited by the free boson and Dirac fermion CFTs, where κ_n decreases with n for $n = 1, 2, 3, 4, \infty$.⁶⁹ The values Eq. (4.25) can be compared with those of the free Dirac fermion:^{48,69} $\kappa_1^{\text{Dirac}} = 0.0722$ and $\kappa_2^{\text{Dirac}} = 0.0472338$, which are 2.5 and 5.6 smaller than for the QBT, respectively. This is in line with the heuristic expectation that κ is a measure of the gapless degrees of freedom since a QBT can be split into a pair of Dirac fermions at different momenta. The splitting can be accomplished by adding a term of the form $A\sigma_z$ to the Hamiltonian Eq. (4.23).

V. FREE RELATIVISTIC THEORIES IN 3 + 1 DIMENSIONS

We now consider the free relativistic complex boson, and 4-component Dirac fermion in three spatial dimensions. Let us consider their groundstate on the three dimensional torus $L_x \times L_y \times L_z$, and take region A to be the cylinder $L_A \times L_y \times L_z$, as shown in Fig. 3. The entanglement entropies will take the following form:

$$S_n = \alpha_n \frac{2L_y L_z}{\epsilon^2} - J_n(u; b_1, b_2) + \dots \quad (5.1)$$

with the two aspect ratios being $b_1 = L_x/L_y$ and $b_2 = L_x/L_z$. We note that there is no logarithm because the entangling surface is not curved. J_n will also depend on the boundary

conditions along the three non-contractible cycles. The function $J_1(u; b_1, b_2) - J_1(1/2; b_1, b_2)$ was studied in Ref. 56 for the free complex boson at fixed boundary conditions and $b_1 = b_2$. Here we focus on the *thin torus limit* of the full $J_n(u; b_1, b_2)$, where L_y and L_z tend toward zero at fixed L_x and L_A :

$$\lim_{L_y, L_z \rightarrow 0} J_n(u; b_1, b_2) = 2\gamma_n^{3d}(r), \quad r = L_y/L_z. \quad (5.2)$$

We shall study the general twist dependence. In the thin torus limit, the Rényi entropies can be obtained by Fourier transforming along y and z , which maps the problem to a sum over massive 1d bosons/fermions. Since $L_y, L_z \ll L_A, L_x$, we have

$$S_n = - \sum_{k_x, k_y} \frac{1}{6} \left(1 + \frac{1}{n} \right) \log[(k_y^2 + k_z^2 + m^2)\epsilon^2] \quad (5.3)$$

where we have used the 1+1-dimensional expression for the EE,⁷⁰ setting the Virasoro central charge to $c = 2$ since we work with a complex boson or a 4-component Dirac fermion. The momenta are quantized as follows: $k_y = 2\pi(n_1 + \lambda_1)/L_y$, $k_z = 2\pi(n_2 + \lambda_2)/L_z$, $n_1, n_2 \in \mathbb{Z}$ and $\lambda_1, \lambda_2 \in (0, 1)$. The case $\lambda_1 = \lambda_2 = 0$ requires special care, and we treat it separately below. To extract the universal subleading correction to the EE, we need to evaluate the double series

$$g(mL_y; \lambda_i, r) = \sum_{n_1, n_2 = -\infty}^{\infty} \log \left[\left(\frac{mL_y}{2\pi} \right)^2 + (n_1 + \lambda_1)^2 + r^2(n_2 + \lambda_2)^2 \right] \quad (5.4)$$

where $r = L_y/L_z$. We consider the massless $m = 0$ and massive $m \neq 0$ cases separately.

A. Massless case

For the conformal state, $m = 0$, the double series of Eq.(5.4) becomes

$$g(0; \lambda_i, r) = \sum_{n_1, n_2 = -\infty}^{\infty} \log [(n_1 + \lambda_1)^2 + r^2(n_2 + \lambda_2)^2] \quad (5.5)$$

As shown in Appendix B 3, this series is given, after regularization, by the expression

$$g(0; \lambda_i, r) = \log \left(\frac{\theta \left[\begin{smallmatrix} \lambda_2 - \frac{1}{2} \\ \lambda_1 - \frac{1}{2} \end{smallmatrix} \right] (\tau)}{\eta(\tau)} \cdot \frac{\theta \left[\begin{smallmatrix} \lambda_2 - \frac{1}{2} \\ -\lambda_1 + \frac{1}{2} \end{smallmatrix} \right] (\tau)}{\eta(\tau)} \right) \quad (5.6)$$

where $\tau = ir = iL_y/L_z$ is the modular parameter of the toroidal boundary. We have assumed $\lambda_1, \lambda_2 > 0$, i.e. we exclude simultaneous periodic boundary conditions along y and z . The

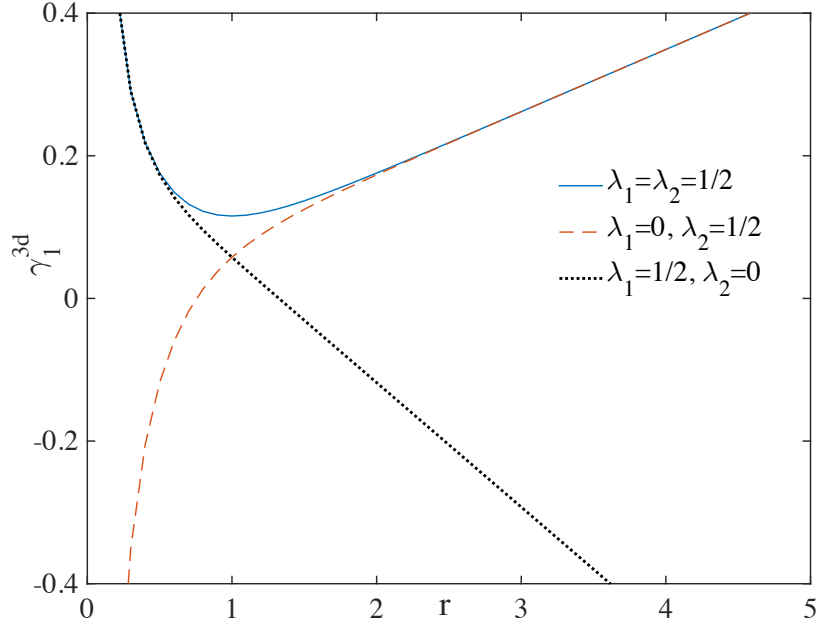


FIG. 11. (Color online) The function γ_1^{3d} for the universal term of the von Neumann EE of a complex massless boson / 4-component Dirac fermion in 3+1 dimensions for a semi-infinite partition of an infinite cylinder. γ_1^{3d} , given in Eq.(5.7), is plotted as a function of the torus aspect ratio $r = L_y/L_z$, and for various values of the twists λ_1 and λ_2 .

$\lambda_1 = \lambda_2 = 0$ case requires special care, as we discuss below. Therefore, in the massless case, the subleading universal term to the EE is (for $\lambda_1, \lambda_2 > 0$)

$$2\gamma_n^{3d} = \frac{1}{6} \left(1 + \frac{1}{n}\right) \log \left(\frac{\theta \left[\begin{smallmatrix} \lambda_2 - \frac{1}{2} \\ \lambda_1 - \frac{1}{2} \end{smallmatrix} \right] (\tau)}{\eta(\tau)} \cdot \frac{\theta \left[\begin{smallmatrix} \lambda_2 - \frac{1}{2} \\ -\lambda_1 + \frac{1}{2} \end{smallmatrix} \right] (\tau)}{\eta(\tau)} \right) \quad (5.7)$$

In the special case $\lambda_1 = \lambda_2$ and $r = 1$, γ_n^{3d} was derived in Ref. 36 for the complex boson, where they used the replica trick method, and expressed the result in terms of the first Jacobi theta function. Eq.(5.7) reduces to their answer when $\lambda_1 = \lambda_2$, as can be seen by using the relation between $\theta \left[\begin{smallmatrix} \alpha \\ \beta \end{smallmatrix} \right] (\tau)$ and the first Jacobi theta function θ_1 , Eq.(B16). We should emphasize that our result in Eq.(5.7) is valid for arbitrary values of the twists λ_i (as long as $\lambda_1, \lambda_2 > 0$) and r , and that it also holds for the Dirac fermion.

Our setup is symmetric under the interchange of the y and z directions, which means that $J_n(1/2)$ is invariant under the simultaneous exchanges $r \leftrightarrow 1/r$ and $\lambda_1 \leftrightarrow \lambda_2$. This symmetry can be seen by taking $\tau \rightarrow -1/\tau$, $\lambda_1 \rightarrow \lambda_2$, $\lambda_2 \rightarrow \lambda_1$ in Eq.(5.6), and using the

relations of Eq. (A3), $\eta(-1/\tau) = \sqrt{-i\tau}\eta(\tau)$, and $\theta\left[\begin{smallmatrix} \alpha \\ -\beta \end{smallmatrix}\right](-1/\tau) = \sqrt{-i\tau}e^{2\pi\alpha\beta}\theta\left[\begin{smallmatrix} \beta \\ -\alpha \end{smallmatrix}\right](\tau)$.

Since the closed form answer Eq. (5.7) is somewhat opaque, we find it useful to examine special limits where γ^{3d} simplifies. For instance when the boundary becomes very elongated in one direction, say $r = L_y/L_z \rightarrow \infty$, we find

$$2\gamma_n^{3d} = -\left(1 + \frac{1}{n}\right) \frac{2\pi r}{3} \left[\frac{1}{2} \left(\lambda_2 - \frac{1}{2}\right)^2 - \frac{1}{24} \right] \quad (5.8)$$

Thus, γ_n^{3d} diverges linearly with r and only depends on the twist in the (short) z direction, λ_2 . This asymptotic behavior is seen in Fig. 11. Conversely, in the opposite limit, $r \rightarrow 0$, we find instead

$$2\gamma_n^{3d} = -\left(1 + \frac{1}{n}\right) \frac{2\pi}{3r} \left[\frac{1}{2} \left(\lambda_1 - \frac{1}{2}\right)^2 - \frac{1}{24} \right] \quad (5.9)$$

In this case, it only depends on the twist in y direction and is independent of λ_2 . We note that Eq. (5.9) can be obtain from Eq. (5.8) by using the symmetry that interchanges the y, z directions. The $1/r$ divergence is shown in Fig. 11.

Fig. 11 shows the full result for γ_1^{3d} as a function of r and different values of λ_1 and λ_2 . Notice that γ_1 can be both negative and positive depending on the value of the twists λ_1 and λ_2 . We see that there is a apparent divergence as $\lambda_1, \lambda_2 \rightarrow 0$, which we now turn to by examining the periodic case $\lambda_1 = \lambda_2 = 0$.

Periodic case, $\lambda_1 = \lambda_2 = 0$: We can no longer use Eq.(5.3) because of the zero mode $k_y = k_z = 0$. The zero mode will contribute a term dependent on $u = L_A/L_x$ and L_x/ϵ where ϵ is the short distance cutoff, as well as on the twist in the x -direction λ_x . This is exactly as for the 2+1d CFTs, and is a consequence of the momentum decomposition of the EE in the free CFTs: $S_n = \sum_{k_y, k_z} S_n^{1d}(k_y, k_z)$, where the transverse momenta determine the effective masses of the 1d modes; we have omitted the dependence on the twist parameters. When $\lambda_1 = \lambda_2 = 0$, the 1d mode with $k_y = k_z = 0$ has zero mass and will dominate the EE. It is exactly the same zero mode encountered in 2+1d, which implies that

$$\gamma_n^{3d}|_{\lambda_1=\lambda_2=0} = \gamma_n^{2d}|_{\lambda=0} + \dots \quad (5.10)$$

where the dots denote a constant independent of L_x, ϵ, λ_x . For periodic boundary conditions along x , $\lambda_x = 0$, we have, see Eq.(3.15),

$$\gamma_n^{3d}|_{\lambda_1=\lambda_2=0} = -\frac{1}{6} \left(1 + \frac{1}{n}\right) \log \left(\frac{L_x}{\pi\epsilon} \sin \left(\frac{\pi L_A}{L_x} \right) \right) + \dots \quad (5.11)$$

For $\lambda_x > 0$, the Rényi entropies for a free boson CFT in 1+1d were analytically computed as a function of λ_x by Shiba⁶⁴, and these have to be used instead of (5.11). For the Dirac fermion, the answer is not known at present. Finally, we note that by turning on a small $\lambda_1, \lambda_2 > 0$, the apparent logarithmic divergence $\log(1/\epsilon)$ will be cutoff, leading to the $\log(\lambda_{1,2})$ scaling seen above.

B. Massive case

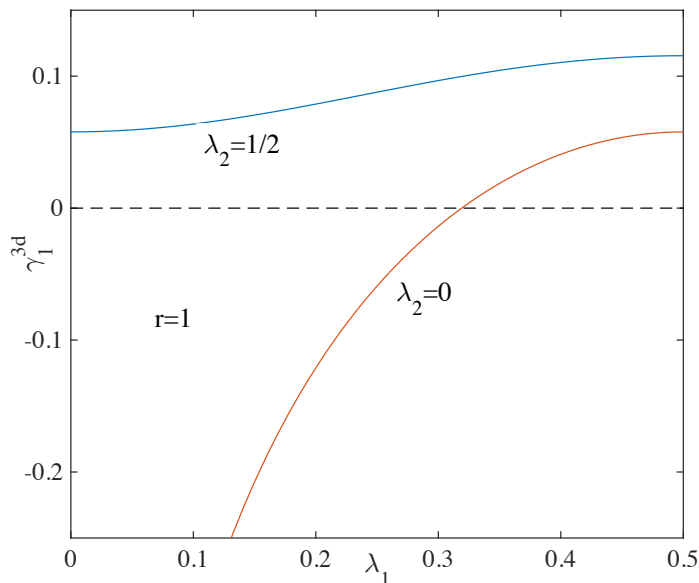


FIG. 12. (Color online) The universal term γ_1^{3d} of the von Neumann EE for a massless complex boson / 4-component Dirac fermion in 3+1 dimensions, Eq. (5.7), plotted as a function of λ_1 for a torus with aspect ratio $r = 1$. The top (bottom) curve corresponds to $\lambda_2 = 1/2$ (0). For $\lambda_2 = 0$, γ_1^{3d} vanishes at $\lambda_1 \simeq 0.319$.

We turn on a finite mass $m > 0$. We work in the thin torus limit $L_y, L_z \ll L_A, L_x$, and study γ^{3d} as function of mL_y and mL_z , and the twists. This means that we keep $mL_{y,z}$ order unity. This is equivalent to working on the semi-infinite cylinder with L_x and L_A infinite (where we would get γ^{3d} instead of $2\gamma^{3d}$). To evaluate the double sum over modes, Eq.(5.4), we can first sum over n_1 . According to Eq.(B9), we have

$$g(mL_y; \lambda_i, r) = g_1(mL_y; \lambda_i, r) + g_2(mL_y; \lambda_i, r) \quad (5.12)$$

where g_1 is given by

$$g_1(mL_y; \lambda_i, r) = 2\pi \sum_{n_2 \in \mathbb{Z}} \sqrt{\left(\frac{mL_y}{2\pi}\right)^2 + r^2(n_2 + \lambda_2)^2}, \quad (5.13)$$

and g_2 by

$$g_2(mL_y; \lambda_i, r) = \sum_{n_2 \in \mathbb{Z}} \log \left[(1 - e^{2\pi i \lambda_1 - 2\sqrt{t}\pi})(1 - e^{-2\pi i \lambda_1 - 2\sqrt{t}\pi}) \right] \quad (5.14)$$

with $t = \left(\frac{mL_y}{2\pi}\right)^2 + r^2(n_2 + \lambda_2)^2$. g_2 is finite but g_1 is divergent and needs to be further regularized. Using the derivation in Appendix B 2, we can separate the divergent and finite contributions to g_1 ,

$$g_1 = -\frac{(mL_y)^2}{4\pi r} \Gamma(-1) - \frac{(mL_y)^2}{\pi r} \sum_{p \neq 0} e^{2\pi i p \lambda_2} \frac{K_1(z)}{z} \quad (5.15)$$

where $z = \frac{mL_y}{r}|p|$, $\Gamma(-1) = \infty$ and $K_\nu(z)$ is the modified Bessel function of the second kind.

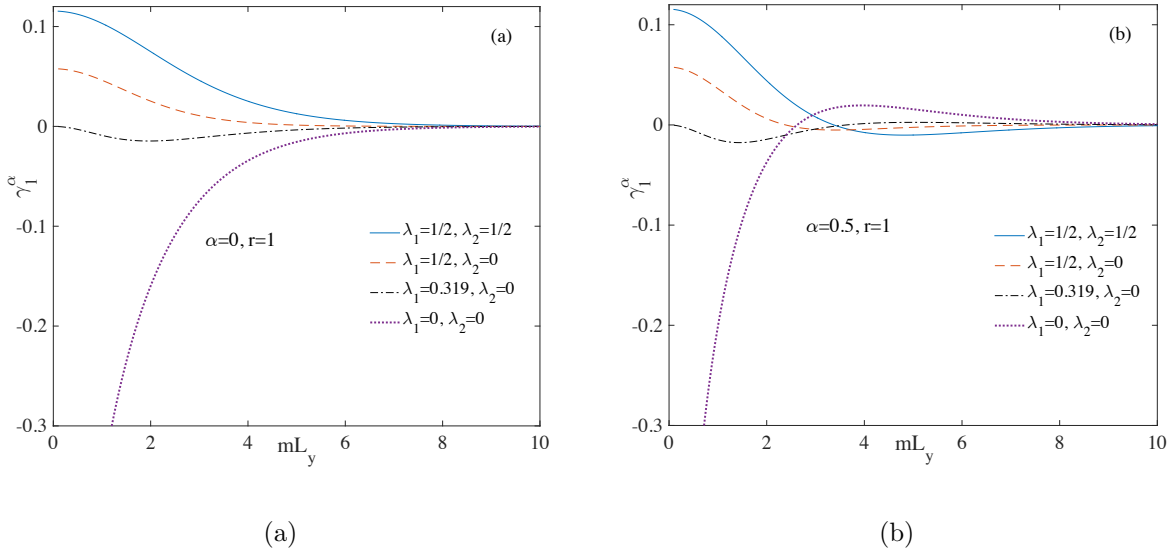


FIG. 13. (Color online) The renormalized von Neumann EE $\gamma_1^{(\alpha)}$, (a) for $\alpha = 0$, and (b) $\alpha = 1/2$, given in Eq.(5.17), for a complex boson / 4-component Dirac fermion of mass m in 3+1 dimensions. It is a scaling function of mL_y , and is shown for four choices of the twists $\lambda_{1,2}$, and fixed torus aspect ratio $r = 1$.

Just as was the case in 2+1 dimensions, we cannot simply subtract the area law in order to obtain a sensible answer for γ_n^{3d} when the mass is finite. Working in the thin torus limit,

we consider the one-parameter family of renormalized EEs:⁶⁶

$$2\gamma_n^{(\alpha)}(mL_y; r) = \frac{1}{2} \left[\alpha L_y^2 \frac{\partial^2 S_n(L_y)}{\partial L_y^2} + (1 - \alpha) L_y \frac{\partial S_n(L_y)}{\partial L_y} - 2S_n(L_y) \right] \quad (5.16)$$

which is the most general form that ensures a cancellation of the area law, is linear in S_n , and includes terms up to second order in L_y -derivatives. The case linear in derivatives, $\alpha = 0$, is the natural analogue of the 2+1 dimensional renormalized EE used above, Eq. (3.18). The aspect ratio $r = L_y/L_z$ is kept as a fixed constant to ensure that the entangling geometry does not change shape as we probe the entanglement along the RG flow parametrized by mL_y . At a scale-invariant fixed point, Eq. (5.16) reduces to $2\gamma_n^{3d}(r)$. In $\gamma_n^{(\alpha)}$, the divergent term in g_1 will cancel and we have

$$2\gamma_n^{(\alpha)}(mL_y) = -\frac{1}{12} \left(1 + \frac{1}{n} \right) \left[\alpha L_y^2 \frac{\partial^2 (\tilde{g}_1 + g_2)}{\partial L_y^2} + (1 - \alpha) L_y \frac{\partial (\tilde{g}_1 + g_2)}{\partial L_y} - 2(\tilde{g}_1 + g_2) \right] \quad (5.17)$$

where \tilde{g}_1 is the finite part of g_1 . We evaluate this expression numerically and plot it in Fig. 13 for $\alpha = 0, 1/2$ and $r = 1$. In the deep IR limit, $mL_y \rightarrow \infty$, $\gamma_1^{(\alpha)}$ eventually approaches zero. The fact that $\gamma = 0$ at the trivial gapped IR fixed point has been discussed in Ref. 71. In most cases, it is not monotonically decreasing with mL_y . Actually, in the massless limit, $\gamma_n^{(\alpha)}(mL_y)$ reduces to Eq.(5.7) by construction. Clearly, it is not possible to define $\gamma_n^{(\alpha)}$ to be a monotonic decreasing function since at $mL_y = 0$ (IR), as shown in Fig. 12, already in the massless limit γ_1^{3d} can take either positive or negative values as a function of the twists λ_1 and λ_2 . In the special case $\lambda_1 \simeq 0.319$ and $\lambda_2 = 0$, γ^{3d} is strictly equal to zero at the massless point, but we find that no matter how we tune α , $\gamma_1^{(\alpha)}(mL_y)$ becomes finite at $mL_y > 0$, which means that it cannot be monotonic since it also approaches zero as $mL_y \rightarrow \infty$. Although $\gamma_1^{(\alpha)}$ is generally not a monotonic function along the RG flow, it is nevertheless a simple and non-trivial entanglement measure that is universal (independent of the UV cutoff).

VI. CONCLUSIONS

In this paper, we investigated the subleading correction term $J_n(u)$ of two-cylinder EE for several scale invariant free systems in both 2 + 1 dimensions and 3 + 1 dimensions. We numerically studied $J_n(u, b)$ under various twisted boundary conditions in 2 + 1 dimensions. In the thin torus limit, we found that $J_n(u, b)$ converges to some constant $2\gamma_n$ which only

depends on the twist and is independent of any length scale of the system. We further evaluated this constant analytically for Dirac fermion CFT, free boson CFT and massless $z = 2$ free boson system and find that they take the same form, as a function of the twist, up to a prefactor. This is in contrast to the fermionic quadratic band touching model, where γ_n is always equal to zero. We further extended our calculations to $3 + 1$ dimensions and obtained the analytical expression for γ_n^{3d} in the thin torus limit for both free boson CFT and Dirac fermion CFT with twisted boundary conditions.

The finite constant terms in the EE contain non-trivial and universal information on the properties of scale-invariant field theories. In addition to providing new insights about these fixed-point theories they may also constrain the allowed RG flows between two fixed points after we deform away from the UV theory. Indeed a long-standing problem is to find possible generalizations of the celebrated Zamolodchikov’s c -theorem of 1+1-dimensional field theories which showed that under the action of a relevant perturbation the relativistic RG flow always connects two fixed points with decreasing values of the conformal central charge c , and that this change is described by a monotonically decreasing c -function along the RG flow.⁷

One of the problems faced in this endeavor is to find a quantity that would play the role similar to that of the central charge of the trace anomaly of the energy momentum tensor.⁶ This quantity is unique only in 1+1-dimensional CFTs and already in 3+1 dimensions there are two such “central charges”, named c and a respectively. In odd space-time dimensions there are no such quantities associated with the energy-momentum tensor. The discovery that in 1+1 dimensional CFTs the central charge c determines the coefficient of the logarithmic term of the EE as well as the demonstration that EE provides a *new* RG monotone has turned the problem of finding generalizations of Zamolodchikov’s theorem to that of finding similar behavior for EE in higher dimensional theories.

In 3+1 dimensional relativistic theories an a -theorem for a central charge has been established.⁷² Here a enters in the logarithmic corrections to the area law term of the EE for a spherical entangling surfaces. In this case the actual c -function has not been proven to be related to an EE along the RG-flow, instead a certain integrated cross section, related to a four point function of the trace of the stress tensor, plays this role. The analog of this result in 2+1 dimensional relativistic CFTs is the F -theorem^{38,42,43} associated with the finite universal corrections to the area law for circular entangling surfaces and of an

associated function defined with respect to the EE which decreases monotonically along RG flows. There are further distinctions between the a -theorem and the F -theorem in that the latter is not obviously related to properties of any known *local* operator and F can count topological degrees of freedom^{19,20} while these do not show up in a .

In this paper we have investigated the RG flow of similar finite universal quantities which exist in the EE for cylindrical cuts of 2+1-dimensional theories on a torus. The goal here was to search in the possible parameter space (including twisted boundary conditions and various geometries) for an RG monotone. The quantities we studied in this paper, just like F , have a more non-local origin as they are also able to capture the contributions of non-local degrees of freedom, such as those in topological field theories²¹ and in scale-invariant theories with compactified fields.^{28,34,61,62} However, we only ended up ruling out various reasonable possibilities since the quantities we study do not obey the sought after monotonicity property. Early attempts to generalize the Zamolodchikov c -theorem using the thermodynamic entropy density (which is a natural physical quantity to use to estimate the number of degrees of freedom) also failed to exhibit a monotonically decreasing behavior.^{73,74}

Moving forward one could now expand the search for RG monotones to other geometries and entangling cuts. There are several reasons why we think this is a useful pursuit. The existence of c -functions from a relativistic point of view is on fairly sound footing in 1+1, 2+1 and 3+1 dimensions albeit without a unified picture in these different dimensions. Perhaps some new entanglement entropy quantity will provide such a unification. Similarly for non-relativistic theories positive results on c -functions are non-existent and filling this gap would likely have deep consequences.

Added Note: After submission of this paper, a preprint⁶⁴ of Noburo Shiba appeared, giving the analytical calculation of the entanglement Rényi entropies in a free boson CFT on a circle in 1+1d as a function of the twist λ_x . This is a lower dimensional analogue of our present analysis in 2+1d and 3+1d. There exists a close connection between our results and the 1+1d result of Shiba in the thin torus limit, as explained in Sections III and V.

ACKNOWLEDGMENTS

We thank Pablo Bueno, Lauren Hayward Sierens, Roger Melko, Subir Sachdev, Noburo Shiba, Alex Thomson, and Seth Whitsitt. This work was supported in part by the National Science Foundation through the grant DMR 1408713 at the University of Illinois (EF). XC was supported by a postdoctoral fellowship from the the Gordon and Betty Moore Foundation, under the EPiQS initiative, Grant GBMF-4304, at the Kavli Institute for Theoretical Physics. WWK was supported by a postdoctoral fellowship and a Discovery Grant from NSERC, by a Canada Research Chair, and by MURI grant W911NF-14-1-0003 from ARO. WWK further acknowledges the hospitality of the Aspen Center for Physics, where part of this work was done, and which is supported by the National Science Foundation through the grant PHY-1066293. TF is supported by the DARPA YFA program, contract D15AP00108.

Appendix A: Useful functions and identities

We define the following function

$$\theta \begin{bmatrix} \alpha \\ \beta \end{bmatrix} (\tau) = \eta(\tau) e^{2\pi i \alpha \beta} q^{\frac{\alpha^2}{2} - \frac{1}{24}} \prod_{n=1}^{\infty} \left(1 + q^{n+\alpha-\frac{1}{2}} e^{2\pi i \beta}\right) \left(1 + q^{n-\alpha-\frac{1}{2}} e^{-2\pi i \beta}\right) \quad (\text{A1})$$

where $q = e^{2\pi i \tau}$, and $\eta(\tau)$ is the Dedekind eta function:

$$\eta(\tau) = q^{\frac{1}{24}} \prod_{n=1}^{\infty} (1 - q^n). \quad (\text{A2})$$

Under the S transformation, $\tau \rightarrow -1/\tau$, we have

$$\theta \begin{bmatrix} \alpha \\ \beta \end{bmatrix} (-1/\tau) = \sqrt{-i\tau} e^{2\pi i \alpha \beta} \theta \begin{bmatrix} \beta \\ -\alpha \end{bmatrix} (\tau) \quad (\text{A3})$$

We also define

$$\begin{aligned} \theta_2(\tau) &\equiv \theta \begin{bmatrix} \frac{1}{2} \\ 0 \end{bmatrix} (\tau) = 2q^{1/8} \prod_{n=1}^{\infty} (1 - q^n)(1 + q^n)^2, \\ \theta_4(\tau) &\equiv \theta \begin{bmatrix} 0 \\ \frac{1}{2} \end{bmatrix} (\tau) = \prod_{n=1}^{\infty} (1 - q^n)(1 - q^{n-\frac{1}{2}})^2 \end{aligned} \quad (\text{A4})$$

which are obtained from the full theta Jacobi functions $\theta_\nu(z, \tau)$ by setting $z = 0$. We note that $\theta \begin{bmatrix} \alpha \\ \beta \end{bmatrix} (\tau)$ can be expressed in terms of the theta Jacobi function $\theta_1(z, \tau)$, as shown in Eq.(B16).

Appendix B: Various zeta functions

The details of these zeta functions can be found in Ref. 75.

1. Hurwitz zeta function

Hurwitz zeta function is defined in this way,

$$\zeta(s, \lambda) = \sum_{n=0}^{\infty} \frac{1}{(n + \lambda)^s} \quad (\text{B1})$$

This is Hurwitz zeta function and it satisfies

$$\zeta'(0, \lambda) = - \sum_{n=0}^{\infty} \log(n + \lambda) = \log \Gamma(\lambda) - \frac{1}{2} \log(2\pi) \quad (\text{B2})$$

Therefore we can regularize the infinite sum

$$\begin{aligned} g(\lambda) &= \sum_{n=-\infty}^{\infty} \log |n + \lambda| = \log \prod_{n=0}^{\infty} (n + \lambda) \prod_{n=0}^{\infty} [n + (1 - \lambda)] \\ &= -\zeta'(0, \lambda) - \zeta'(0, 1 - \lambda) \\ &= -\log \Gamma(\lambda) + \frac{1}{2} \log(2\pi) - \log \Gamma(1 - \lambda) + \frac{1}{2} \log(2\pi) \\ &= -\log [\Gamma(\lambda)\Gamma(1 - \lambda)] + \log(2\pi) \\ &= \log(2 \sin(\pi\lambda)) \end{aligned} \quad (\text{B3})$$

where in the last step, we used $\Gamma(\lambda)\Gamma(1 - \lambda) = \pi/\sin(\pi\lambda)$.

2. Epstein zeta function in $d = 1$

Define

$$\begin{aligned} f(s, \lambda, c, \alpha) &= \sum_{n=-\infty}^{\infty} \left[\frac{1}{c + \alpha(n + \lambda)^2} \right]^s \\ &= \frac{1}{\Gamma(s)} \sum_{-\infty}^{\infty} \int_0^{\infty} dt t^{s-1} e^{-t[c + \alpha(n + \lambda)^2]} \\ &= \frac{\sqrt{\pi/\alpha}}{\Gamma(s)} \sum_{-\infty}^{\infty} \int_0^{\infty} dt t^{s-\frac{3}{2}} e^{-\frac{\pi^2}{\alpha t} n^2 - ct + 2\pi i \lambda n} \end{aligned} \quad (\text{B4})$$

where we use

$$\begin{aligned}\Gamma(s) &= \int_0^\infty dx x^{s-1} e^{-x} \\ \sum_{n \in \mathbb{Z}} e^{-\pi a n^2 + b n} &= \frac{1}{\sqrt{a}} \sum_{k \in \mathbb{Z}} e^{-\frac{\pi}{a} (k + \frac{b}{2\pi i})^2}\end{aligned}\tag{B5}$$

with $a = \frac{\pi}{\alpha t}$ and $b = 2\pi i \lambda$.

The $n = 0$ part gives

$$f^{(n=0)}(s, \lambda, c, \alpha) = \frac{\sqrt{\pi/\alpha} \Gamma(s - \frac{1}{2})}{c^{s-\frac{1}{2}} \Gamma(s)}\tag{B6}$$

For $n \neq 0$, we have

$$\begin{aligned}f^{n \neq 0}(s, \lambda, c, \alpha) &= \frac{\sqrt{\pi/\alpha}}{\Gamma(s)} \sum_{n \neq 0} e^{2\pi i \lambda n} \int_0^\infty \frac{dt}{c^{s-\frac{1}{2}}} t^{s-\frac{3}{2}} e^{-t - \frac{c\pi^2 n^2}{\alpha t}} \\ &= \frac{2c^{-s+\frac{1}{2}} \sqrt{\pi/\alpha}}{\Gamma(s)} \sum_{n \neq 0} e^{2\pi i \lambda n} \left(\frac{z}{2}\right)^{s-\frac{1}{2}} K_\nu(z)\end{aligned}\tag{B7}$$

where $K_\nu(z)$ is the modified Bessel function of the second kind

$$K_\nu(z) = \frac{1}{2} \left(\frac{z}{2}\right)^\nu \int_0^\infty dt e^{-t - \frac{z^2}{4t}} t^{-\nu-1}\tag{B8}$$

where $\nu = -s + \frac{1}{2}$ and $z = 2\sqrt{c/\alpha\pi}|n|$. $K_\nu(z) = \sqrt{\frac{\pi}{2z}} e^{-z} + \dots$ Around $s = 0$, $\Gamma(s) \sim 1/s$.

We expand $f(s, \lambda, c, \alpha)$ around $s = 0$,

$$\begin{aligned}f(s \rightarrow 0, \lambda, c, \alpha) &= \frac{\Gamma(s - \frac{1}{2})}{\Gamma(s)} \frac{\sqrt{\pi}}{(c/\alpha)^{-\frac{1}{2}}} + s \sum_{n \neq 0} \frac{e^{2\pi i \lambda n}}{|n|} e^{-2\sqrt{c/\alpha\pi}|n|} \\ &= -2\pi s (c/\alpha)^{\frac{1}{2}} - s \log \left[(1 - e^{2\pi i \lambda - 2\sqrt{c/\alpha\pi}})(1 - e^{-2\pi i \lambda - 2\sqrt{c/\alpha\pi}}) \right]\end{aligned}\tag{B9}$$

where we use $\Gamma(-1/2) = -2\sqrt{\pi}$ and $\log(1-x) = -\sum_{k=1}^\infty x^k/k$.

3. Epstein zeta function in $d = 2$

We define the following double series

$$g(\lambda) = \sum_{n_1, n_2 \in \mathbb{Z}} \log \left[(n_1 + \lambda_1)^2 + r^2 (n_2 + \lambda_2)^2 \right]\tag{B10}$$

To regularize the above equation, we define

$$f(s, \lambda) = \sum_{n_1, n_2 \in \mathbb{Z}} \left[\frac{1}{(n_1 + \lambda_1)^2 + r^2 (n_2 + \lambda_2)^2} \right]^s\tag{B11}$$

Here we first sum over n_1 . According to the result in Eq.(B9), around $s = 0$, we have

$$f(s \rightarrow 0, \lambda) = \sum_{n_2=-\infty}^{\infty} \frac{\Gamma(s - \frac{1}{2})}{\Gamma(s)} \frac{\sqrt{\pi}}{c^{s-\frac{1}{2}}} - \sum_{n_2=-\infty}^{\infty} s \log \left[(1 - e^{2\pi i \lambda_1 - 2\sqrt{c}\pi})(1 - e^{-2\pi i \lambda_1 - 2\sqrt{c}\pi}) \right] \quad (\text{B12})$$

where $\sqrt{c} = |n_2 + \lambda_2|r$.

Hence

$$\begin{aligned} f(s \rightarrow 0, \lambda) &= -s \sum_{n_2=-\infty}^{\infty} \log \left[(1 - e^{2\pi i \lambda_1 - 2r|n_2 + \lambda_2|\pi})(1 - e^{-2\pi i \lambda_1 - 2r|n_2 + \lambda_2|\pi}) \right] \\ &+ \frac{r\sqrt{\pi}\Gamma(s - \frac{1}{2})}{\Gamma(s)} \left[\sum_{n_2=0}^{\infty} \frac{1}{(n_2 + \lambda_2)^{2s-1}} + \sum_{n_2=0}^{\infty} \frac{1}{(n_2 + 1 - \lambda_2)^{2s-1}} \right] \\ &= -s \sum_{n_2>0} \log \left[(1 - e^{2\pi i \lambda_1 - 2r(n_2 + \lambda_2 - 1)\pi})(1 - e^{2\pi i \lambda_1 - 2r(n_2 - \lambda_2)\pi}) \right. \\ &\quad \times \left. (1 - e^{-2\pi i \lambda_1 - 2r(n_2 + \lambda_2 - 1)\pi})(1 - e^{-2\pi i \lambda_1 - 2r(n_2 - \lambda_2)\pi}) \right] - 2rs\pi [\zeta(2s - 1, \lambda_2) + \zeta(2s - 1, 1 - \lambda_2)] \\ &= -s \sum_{n_2>0} \log \left[(1 - e^{2\pi i \lambda_1 - 2r(n_2 + \lambda_2 - 1)\pi})(1 - e^{2\pi i \lambda_1 - 2r(n_2 - \lambda_2)\pi}) \right. \\ &\quad \times \left. (1 - e^{-2\pi i \lambda_1 - 2r(n_2 + \lambda_2 - 1)\pi})(1 - e^{-2\pi i \lambda_1 - 2r(n_2 - \lambda_2)\pi}) \right] + 2rs\pi(\lambda_2^2 - \lambda_2 + \frac{1}{6}) \end{aligned} \quad (\text{B13})$$

where $\zeta(s, x)$ is the Hurwitz zeta function

$$\zeta(s, x) = \sum_{n=0}^{\infty} \frac{1}{(n+x)^s}, \quad \zeta(-1, x) = -\frac{x^2 - x + \frac{1}{6}}{2} \quad (\text{B14})$$

Therefore

$$g(\lambda) = -f'(s, \lambda)|_{s=0} = \log \left\{ \frac{\theta \left[\begin{smallmatrix} \lambda_2 - \frac{1}{2} \\ \lambda_1 - \frac{1}{2} \end{smallmatrix} \right] (\tau)}{\eta(\tau)} \frac{\theta \left[\begin{smallmatrix} \lambda_2 - \frac{1}{2} \\ -\lambda_1 + \frac{1}{2} \end{smallmatrix} \right] (\tau)}{\eta(\tau)} \right\} \quad (\text{B15})$$

where $\tau = ir$, $q = e^{2\pi i \tau}$. The above theta-function in the above equation is related with the first elliptic theta function in the following way,

$$\begin{aligned} \frac{\theta \left[\begin{smallmatrix} \lambda_2 - \frac{1}{2} \\ \lambda_1 - \frac{1}{2} \end{smallmatrix} \right] (\tau)}{\eta(\tau)} &= e^{2\pi i(\lambda_2 - \frac{1}{2})(\lambda_1 - \frac{1}{2})} e^{\pi i \tau(\lambda_2^2 - \lambda_2 + \frac{1}{6})} \prod_{n=1}^{\infty} (1 - q^{n-1} e^{2\pi i(\lambda_1 + \lambda_2 \tau)})(1 - q^n e^{-2\pi i(\lambda_1 + \lambda_2 \tau)}) \\ &= i e^{2\pi i(\lambda_2 - \frac{1}{2})(\lambda_1 - \frac{1}{2})} e^{\pi i \tau \lambda_2^2 + \pi i \lambda_1} \left[-i e^{\pi i z} q^{\frac{1}{12}} \prod_{n=1}^{\infty} (1 - q^n e^{2\pi i z})(1 - q^{n-1} e^{-2\pi i z}) \right] \\ &= i e^{2\pi i(\lambda_2 - \frac{1}{2})(\lambda_1 - \frac{1}{2})} e^{\pi i \tau \lambda_2^2 + \pi i \lambda_1} \frac{\theta_1(z, \tau)}{\eta(\tau)} \end{aligned} \quad (\text{B16})$$

where $z = -(\lambda_1 + \lambda_2 \tau)$, and $\theta_1(z, \tau)$ is the first Jacobi theta function.

Appendix C: Free boson partition function on the cylinder & torus

1. Torus

a. Periodic boundary conditions in x & y directions

Here we follow the method described in Chapter 10.2 of Ref. 76. The partition function for non-compact free boson on the torus without the zero-mode is

$$\begin{aligned}
 Z &= \int [d\varphi] \sqrt{A} \delta \left(\int d^2x \varphi \varphi_0 \right) \exp \left(-\frac{1}{2} \int d^2x (\nabla \varphi)^2 \right) \\
 &= \sqrt{A} \int \prod_n dc_n \exp \left(-\frac{1}{2} \sum_n \omega_n c_n^2 \right) \\
 &= \sqrt{A} \prod_n \left(\frac{2\pi}{\omega_n} \right)^{1/2}
 \end{aligned} \tag{C1}$$

where $A = L_x L_y$ is the area of the torus, and $\varphi_0 = 1/\sqrt{A}$ is the normalized eigenfunction of the zero-mode. We have expanded the field in terms of the eigenfunctions of the Laplacian operator, $\varphi = \sum_n c_n \phi_n(x)$, with corresponding eigenvalues ω_n . We define

$$G(s) = \sum_{n, \omega_n \neq 0} \frac{1}{\omega_n^s} \tag{C2}$$

It satisfies

$$\frac{d}{ds} G(s) = - \sum_n \log(\omega_n) \frac{1}{\omega_n^s} \tag{C3}$$

Therefore we have

$$Z(\tau) = \sqrt{A} \exp \left(\frac{1}{2} G'(0) \right) \tag{C4}$$

The eigenvalues $\omega_{n,m}$ are labeled by k_x and k_y ,

$$\omega_{n,m} = k_x^2 + k_y^2 \tag{C5}$$

with $k_x = \frac{2\pi n}{L_x}$ and $k_y = \frac{2\pi m}{L_y}$. Hence

$$\begin{aligned}
 \left| \frac{2\pi L_x}{A} \right|^{2s} G(s) &= \sum_{(m,n) \neq (0,0)} \frac{1}{|m + n\tilde{\tau}|^{2s}} \\
 &= \sum_{m \neq 0} \frac{1}{|m|^{2s}} + \sum_{n \neq 0} \left(\sum_m \frac{1}{|m + n\tilde{\tau}|^{2s}} \right) \\
 &= 2\zeta(2s) + \sum_{n \neq 0} \left(\sum_m \frac{1}{|m + n\tilde{\tau}|^{2s}} \right)
 \end{aligned} \tag{C6}$$

where $\zeta(z)$ is the Riemann ζ function, $\tilde{\tau} = -1/\tau$ and $\tau = iL_x/L_y$. Here τ is a pure imaginary number. For the second term, using the result in Sec.B 2, when $s \rightarrow 0$, we have

$$\begin{aligned} \sum_{n \neq 0} \sum_m \frac{1}{|m + n\tilde{\tau}|^{2s}} &= -s \sum_{n \neq 0} \left\{ 2\pi|n| \text{Im} \tilde{\tau} + \log \left[(1 - e^{-2\pi|n| \text{Im} \tilde{\tau}})(1 - e^{-2\pi|n| \text{Im} \tilde{\tau}}) \right] \right\} \\ &= -2 \log |\eta(\tilde{\tau})|^2 \end{aligned} \quad (\text{C7})$$

where we use $\zeta(-1) = -1/12$. $\eta(\tau)$ function is defined as

$$\eta(\tau) = q^{\frac{1}{24}} \prod_{n=1}^{\infty} (1 - q^n) \quad (\text{C8})$$

where $q = e^{2\pi i \tau}$.

After including the first term in $G(s)$ and using $\zeta(0) = -\frac{1}{2}$, we have

$$G'(0) = -2 \log \left(\sqrt{A \text{Im} \tilde{\tau}} |\eta(\tilde{\tau})|^2 \right) \quad (\text{C9})$$

Therefore the free boson partition function is

$$Z_{bos}(\tau) = \sqrt{A} \exp \left(\frac{1}{2} G'(0) \right) = \frac{1}{\sqrt{\text{Im} \tilde{\tau}} |\eta(\tilde{\tau})|^2} = \frac{1}{\sqrt{\text{Im} \tau} |\eta(\tau)|^2} \quad (\text{C10})$$

In the last step, we used the S transformation of the $\eta(\tau)$ function.

b. Twist boundary condition

If we impose a twisted boundary condition in the x or y direction, the eigenvalues $\omega_{m,n}$ will be modified,

$$\omega_{n,m} = \left(\frac{2\pi(n + \lambda_1)}{L_x} \right)^2 + \left(\frac{2\pi(m + \lambda_2)}{L_y} \right)^2 \quad (\text{C11})$$

where $\lambda_{1,2}$ are the twists along the x and y directions. After considering the twist boundary condition, there is no zero mode anymore and we have

$$\left| \frac{2\pi L_x}{A} \right|^{2s} G(s) = \sum_{m,n \in \mathbb{Z}} \frac{1}{|m + \lambda_2 + (n + \lambda_1)\tilde{\tau}|^{2s}} \quad (\text{C12})$$

Using the results in Sec.B 2, we have

$$\begin{aligned} \log Z &= -\frac{1}{2} \log \left\{ \frac{\theta \left[\begin{smallmatrix} \lambda_1 - \frac{1}{2} \\ \lambda_2 - \frac{1}{2} \end{smallmatrix} \right] (\tilde{\tau}) \theta \left[\begin{smallmatrix} \lambda_1 - \frac{1}{2} \\ -\lambda_2 + \frac{1}{2} \end{smallmatrix} \right] (\tilde{\tau})}{\eta(\tilde{\tau}) \eta(\tilde{\tau})} \right\} \\ &= -\frac{1}{2} \log \left\{ \frac{\theta \left[\begin{smallmatrix} \lambda_2 - \frac{1}{2} \\ -\lambda_1 + \frac{1}{2} \end{smallmatrix} \right] (\tau) \theta \left[\begin{smallmatrix} -\lambda_2 + \frac{1}{2} \\ -\lambda_1 + \frac{1}{2} \end{smallmatrix} \right] (\tau)}{\eta(\tau) \eta(\tau)} \right\} \end{aligned} \quad (\text{C13})$$

To obtain this result, we perform S transformation $\tau \rightarrow -1/\tau$ in the second step.

2. Open cylinder

a. Periodic in the y direction

For the cylinder, if we impose Dirichlet boundary at two boundaries with $\phi(x = 0) = \phi(x = L_x) = 0$, only half of the modes will remain,

$$\begin{aligned} \left| \frac{2\pi L_x}{A} \right|^{2s} G(s) &= \sum_{m \in \mathbb{Z}, n > 0} \frac{1}{|m + \frac{n\tilde{\tau}}{2}|^{2s}} \\ &= \sum_{n > 0} \left(\sum_{m \in \mathbb{Z}} \frac{1}{|m + \frac{n\tilde{\tau}}{2}|^{2s}} \right) \end{aligned} \quad (\text{C14})$$

Using the zeta function regularization technique, we expand $G(s)$ around $s = 0$,

$$G(s) = \frac{1}{6} s \pi \frac{\text{Im } \tilde{\tau}}{2} - s \prod_{n > 0} \log \left[(1 - e^{2\pi i n \frac{\tilde{\tau}}{2}})^2 \right] + \dots = -s \log (|\eta(\tilde{\tau}/2)|^2) + \dots \quad (\text{C15})$$

where the dots denote higher order terms in s .

Hence

$$Z_{cyl}(\tau) = \exp \left(\frac{1}{2} G'(0) \right) = \frac{1}{\eta(-\frac{1}{2\tau})} = \frac{1}{\sqrt{-2i\tau} \eta(2\tau)} \quad (\text{C16})$$

b. Twisted boundary condition in the y direction

In this case, we need to calculate

$$\begin{aligned} \left| \frac{2\pi L_x}{A} \right|^{2s} G(s) &= \sum_{m \in \mathbb{Z}, n > 0} \frac{1}{|m + \lambda + \frac{n\tilde{\tau}}{2}|^{2s}} \\ &= \sum_{n > 0} \left(\sum_{m \in \mathbb{Z}} \frac{1}{|m + \lambda + \frac{n\tilde{\tau}}{2}|^{2s}} \right) \end{aligned} \quad (\text{C17})$$

Expanding $G(s)$ around $s = 0$, we have

$$G(s) = \frac{1}{6} s \pi \frac{\text{Im } \tilde{\tau}}{2} - s \prod_{n > 0} \log \left[(1 - e^{2\pi i \lambda + 2\pi i n \frac{\tilde{\tau}}{2}}) (1 - e^{-2\pi i \lambda + 2\pi i n \frac{\tilde{\tau}}{2}}) \right] \quad (\text{C18})$$

Therefore the partition function is

$$\begin{aligned}
Z &= \tilde{q}^{-1/24} \prod_{n=1}^{\infty} \sqrt{\frac{1}{(1 - e^{2\pi i \lambda \tilde{q}^n})(1 - e^{-2\pi i \lambda \tilde{q}^n})}} \\
&= e^{\frac{\pi i}{2}(\lambda - \frac{1}{2})} \sqrt{(1 - e^{-2\pi i \lambda})} \sqrt{\frac{\eta(-\frac{1}{2\tau})}{\theta\left[\frac{\frac{1}{2}}{\lambda - \frac{1}{2}}\right](-\frac{1}{2\tau})}} \\
&= \sqrt{(1 - e^{-2\pi i \lambda})} \sqrt{\frac{\eta(2\tau)}{\theta\left[\frac{\lambda - \frac{1}{2}}{-\frac{1}{2}}\right](2\tau)}} \tag{C19}
\end{aligned}$$

where $\tilde{q} = e^{2\pi i \left(\frac{1}{-2\tau}\right)}$, $\tau = i \frac{L_x}{L_y}$, $q = e^{2\pi i \tau}$.

For instance, if we impose anti-periodic boundary condition in y direction with $\lambda = 1/2$, the partition function becomes

$$Z = \sqrt{2} \sqrt{\frac{\eta(-\frac{1}{2\tau})}{\theta_2(-\frac{1}{2\tau})}} = \sqrt{2} \sqrt{\frac{\eta(2\tau)}{\theta_4(2\tau)}} = \sqrt{2} q^{\frac{1}{24}} \prod_{n=1}^{\infty} \frac{1}{(1 - q^{2n-1})} \tag{C20}$$

Appendix D: Numerical method for calculating EE in free systems

1. Free scalar field theory

The discrete free boson Hamiltonian defined on a lattice reads

$$H = \frac{1}{2} \left(\sum_{i=1}^N \Pi_i^2 + \sum_{i,j=1}^N \phi_i K_{ij} \phi_j \right) \tag{D1}$$

where K_{ij} is a discretized version of $-\nabla^2 + m^2$. The operators satisfy the canonical commutation relations

$$[\phi_i, \Pi_j] = i\delta_{ij}, \quad [\phi_i, \phi_j] = 0, \quad [\Pi_i, \Pi_j] = 0 \tag{D2}$$

The ground state for this Hamiltonian is

$$|\Psi\rangle = \mathcal{N} \sum_{\varphi} e^{-\frac{1}{2} \sum_{ij} \varphi_i K_{ij}^{1/2} \varphi_j} |\varphi\rangle \tag{D3}$$

where $\varphi = \{\varphi_i\}$ denotes a field configuration, and $\phi_i |\varphi\rangle = \varphi_i |\varphi\rangle$, and \mathcal{N} is a normalization. We use this wavefunction to calculate the entanglement entropy. For free boson system, there is a very efficient numerical method to calculate the entanglement entropy. Below is a short summary of the method, while the details can be found in Ref. 48.

The correlation functions for the ground state are

$$\begin{aligned}\langle \phi_i \phi_j \rangle &= \frac{1}{2} K_{ij}^{-1/2} \equiv X_{ij} \\ \langle \pi_i \pi_j \rangle &= \frac{1}{2} K_{ij}^{1/2} \equiv P_{ij}\end{aligned}\tag{D4}$$

The von Neumann EE for subsystem A can be calculated by using these correlation functions,

$$S_1(A) = \sum_{\ell} \left(\nu_{\ell} + \frac{1}{2} \right) \log \left(\nu_{\ell} + \frac{1}{2} \right) - \left(\nu_{\ell} - \frac{1}{2} \right) \log \left(\nu_{\ell} - \frac{1}{2} \right)\tag{D5}$$

where the ν_{ℓ} are eigenvalues of $C = \sqrt{X_A P_A}$. X_A and P_A are the correlation functions defined on subregion A . Similarly, the Rényi EE for $n > 0$ reads

$$S_n = \sum_{\ell} \frac{1}{n-1} \left[\log \left(\left(\nu_{\ell} + \frac{1}{2} \right)^n - \left(\nu_{\ell} - \frac{1}{2} \right)^n \right) \right].\tag{D6}$$

a. Relativistic boson in 2 + 1d

The Hamiltonian for the relativistic boson in 2 + 1d is

$$H = \frac{1}{2} \int d^2x \left[\Pi^2 + (\nabla \phi)^2 + m^2 \phi^2 \right]\tag{D7}$$

The corresponding discrete lattice Hamiltonian (on the torus) is

$$H = \frac{1}{2} \sum_{i,j} \left[\Pi_{i,j}^2 + (\phi_{i+1,j} - \phi_{i,j})^2 + (\phi_{i,j+1} - \phi_{i,j})^2 + m^2 \phi_{i,j}^2 \right]\tag{D8}$$

In the momentum space, the Hamiltonian becomes

$$H = \frac{1}{2} \int_{-\pi}^{\pi} dk_1 \int_{-\pi}^{\pi} dk_2 \Pi(k) \Pi(-k) + [4 - 2 \cos(k_1) - 2 \cos(k_2) + m^2] \phi(k) \phi(-k)\tag{D9}$$

The two point correlation functions are

$$\begin{aligned}\langle \phi_{i,j} \phi_{i+n_1,j+n_2} \rangle &= \frac{1}{8\pi^2} \int_{-\pi}^{\pi} dk_1 \int_{-\pi}^{\pi} dk_2 \frac{\cos(k_1 n_1) \cos(k_2 n_2)}{\sqrt{4 - 2 \cos(k_1) - 2 \cos(k_2) + m^2}} \\ \langle \pi_{i,j} \pi_{i+n_1,j+n_2} \rangle &= \frac{1}{8\pi^2} \int_{-\pi}^{\pi} dk_1 \int_{-\pi}^{\pi} dk_2 \cos(k_1 n_1) \cos(k_2 n_2) \sqrt{4 - 2 \cos(k_1) - 2 \cos(k_2) + m^2}\end{aligned}\tag{D10}$$

we can use these correlation functions to construct C matrix and calculate EE.

2. Numerical method for the free Dirac fermion in 2 + 1 dimensions

Here we follow the method in Ref. 78 and show a simple example for massless Dirac fermion. The Hamiltonian in the momentum space is

$$H_D = \int_{BZ} \frac{d^2k}{(2\pi)^2} \Psi^\dagger(\mathbf{k}) \mathcal{H}_D(\mathbf{k}) \Psi(\mathbf{k}) \quad (\text{D11})$$

where $\Psi^\dagger(\mathbf{k}) = (c_{\mathbf{k}}^\dagger, d_{\mathbf{k}}^\dagger)$ is a two component spinor, BZ stands for the first Brillouin zone, $-\pi < k_x \leq \pi$ and $-\pi < k_y \leq \pi$. The one-particle lattice Dirac Hamiltonian $\mathcal{H}_D(\mathbf{k})$ takes this form

$$\mathcal{H}_D(\mathbf{k}) = h_1 \sigma_x + h_3 \sigma_z \quad (\text{D12})$$

with $h_1 = \cos(k_x)$ and $h_3 = \cos(k_y)$. The Dirac points are at $(\pm\pi/2, \pm\pi/2)$ and there are four Dirac cones in the first Brillouin zone.

$\mathcal{H}_D(\mathbf{k})$ can be diagonalized by a unitary transformation $V^{-1} \mathcal{H}_D V = M$ where M is the diagonal matrix with eigenvalues $E(\mathbf{k})_{\pm} = \pm \sqrt{\cos(k_x)^2 + \cos(k_y)^2}$. The V matrix equals to

$$V = \frac{1}{\sqrt{(2 \cos(k_y)^2 + 2 \cos(k_x)^2 - 2 \cos(k_y) \sqrt{\cos(k_y)^2 + \cos(k_x)^2})^2}} \times \begin{pmatrix} \cos(k_x) & -\cos(k_y) + \sqrt{\cos(k_y)^2 + \cos(k_x)^2} \\ -\cos(k_y) + \sqrt{\cos(k_y)^2 + \cos(k_x)^2} & -\cos(k_x) \end{pmatrix} \quad (\text{D13})$$

For the ground state with lower band fully filled, the correlation functions in momentum space equal to

$$\langle c_{\mathbf{k}}^\dagger c_{\mathbf{k}} \rangle = V_{12}^2, \quad \langle d_{\mathbf{k}}^\dagger d_{\mathbf{k}} \rangle = V_{22}^2, \quad \langle c_{\mathbf{k}}^\dagger d_{\mathbf{k}} \rangle = V_{12} V_{22} \quad (\text{D14})$$

Using the above equations, we can construct the correlation function matrix C_E for the subsystem A and therefore the von Neumann EE is

$$S_{vN} = - \sum_{\ell} [\nu_{\ell} \log \nu_{\ell} + (1 - \nu_{\ell}) \log(1 - \nu_{\ell})] \quad (\text{D15})$$

where ν_{ℓ} is the eigenvalue for C_E . Similarly, the Rényi entropy is

$$S_n = \frac{1}{1-n} \sum_{\ell} \log [(1 - \nu_{\ell})^n + \nu_{\ell}^n] \quad (\text{D16})$$

* xchen@kitp.ucsb.edu

† w.witczak-krempa@umontreal.ca

‡ tomf@illinois.edu

§ efradkin@illinois.edu

- ¹ C. Callan and F. Wilczek, *Physics Letters B* **333**, 55 (1994).
- ² C. Holzhey, F. Larsen, and F. Wilczek, *Nuclear Physics B* **424**, 443 (1994).
- ³ P. Calabrese and J. Cardy, *Journal of Statistical Mechanics: Theory and Experiment* **2004**, P06002 (2004).
- ⁴ G. Vidal, J. L. Latorre, E. Rico, and A. Kitaev, *Physical Review Letters* **90**, 227902 (2003).
- ⁵ P. Calabrese, J. Cardy, and E. Tonni, *Journal of Statistical Mechanics: Theory and Experiment* **2011**, P01021 (2011).
- ⁶ J. L. Cardy, *Physics Letters B* **215**, 749 (1988).
- ⁷ A. B. Zamolodchikov, *Pis'ma Zh. Eksp. Teor. Fiz.* **43**, 565 (1986), (*JETP Lett.* **43**, 730 (1986)).
- ⁸ M. Srednicki, *Physical Review Letters* **71**, 666 (1993).
- ⁹ L. Bombelli, R. K. Koul, J. Lee, and R. D. Sorkin, *Physical Review D* **34**, 373 (1986).
- ¹⁰ J. D. Bekenstein, *Physical Review D* **7**, 2333 (1973).
- ¹¹ S. W. Hawking, *Communications in Mathematical Physics* **43**, 199 (1975).
- ¹² S. Ryu and T. Takayanagi, *Physical Review Letters* **96**, 181602 (2006).
- ¹³ S. Ryu and T. Takayanagi, *Journal of High Energy Physics* **0608**, 045 (2006).
- ¹⁴ D. V. Fursaev, *Physical Review D* **73**, 124025 (2006).
- ¹⁵ S. N. Solodukhin, *Physics Letters B* **665**, 305 (2008).
- ¹⁶ H. Casini and M. Huerta, *Physics Letters B* **694**, 167 (2010).
- ¹⁷ H. Casini, M. Huerta, and R. C. Myers, *Journal of High Energy Physics* **2011**, 036 (2011).
- ¹⁸ E. Witten, *Commun. Math. Phys.* **121**, 351 (1989).
- ¹⁹ A. Kitaev and J. Preskill, *Physical Review Letters* **96**, 110404 (2006).
- ²⁰ M. Levin and X.-G. Wen, *Physical Review Letters* **96**, 110405 (2006).
- ²¹ S. Dong, E. Fradkin, R. G. Leigh, and S. Nowling, *Journal of High Energy Physics* **05**, 016 (2008).
- ²² E. Ardonne, P. Fendley, and E. Fradkin, *Annals of Physics* **310**, 493 (2004).
- ²³ D. Rokhsar and S. A. Kivelson, *Physical Review Letters* **61**, 2376 (1988).
- ²⁴ R. Moessner, S. L. Sondhi, and E. Fradkin, *Physical Review B* **65**, 024504 (2001).
- ²⁵ E. Fradkin, D. Huse, R. Moessner, V. Oganesyan, and S. L. Sondhi, *Physical Review B* **69**,

- 224415 (2004).
- ²⁶ C. Castelnovo, C. Chamon, C. Mudry, and P. Pujol, *Annals of Physics* **318**, 316 (2004).
- ²⁷ E. Fradkin and J. E. Moore, *Physical Review Letters* **97**, 050404 (2006).
- ²⁸ B. Hsu, M. Mulligan, E. Fradkin, and E.-A. Kim, *Physical Review B* **79**, 115421 (2009).
- ²⁹ J.-M. Stephan, S. Furukawa, G. Misguich, and V. Pasquier, *Physical Review B* **80**, 184421 (2009).
- ³⁰ B. Hsu and E. Fradkin, *Journal of Statistical Mechanics: Theory and Experiment* **2010**, P09004 (2010).
- ³¹ M. Oshikawa, *Boundary Conformal Field Theory and Entanglement Entropy in Two-Dimensional Quantum Lifshitz Critical Point* (2010), arXiv: 1007.3739.
- ³² J.-M. Stephan, G. Misguich, and V. Pasquier, *Journal of Statistical Mechanics: Theory and Experiment* **2012**, P02003 (2012).
- ³³ J.-M. Stephan, H. Ju, P. Fendley, and R. G. Melko, *New Journal of Physics* **15**, 015004 (2013).
- ³⁴ T. Zhou, X. Chen, T. Faulkner, and E. Fradkin, *Journal of Statistical Mechanics: Theory and Experiment* **2016**, 093101 (2016).
- ³⁵ M. P. Zaletel, J. H. Bardarson, and J. E. Moore, *Physical Review Letters* **107**, 020402 (2011).
- ³⁶ M. A. Metlitski, C. A. Fuertes, and S. Sachdev, *Physical Review B* **80**, 115122 (2009).
- ³⁷ S. Whitsitt, W. Witczak-Krempa, and S. Sachdev, *Entanglement entropy of the large N Wilson-Fisher conformal field theory* (2016), arXiv:1610.06568.
- ³⁸ H. Casini and M. Huerta, *Phys. Rev. D* **85**, 125016 (2012).
- ³⁹ H. Casini, M. Huerta, R. C. Myers, and A. Yale, *Journal of High Energy Physics* **2015**, 3 (2015).
- ⁴⁰ H. Liu and M. Mezei, *Journal of High Energy Physics* **2013**, 162 (2013).
- ⁴¹ R. C. Myers and A. Sinha, *Phys. Rev. D* **82**, 046006 (2010).
- ⁴² D. L. Jafferis, I. R. Klebanov, S. S. Pufu, and B. R. Safdi, *Journal of High Energy Physics* **1106**, 106 (2011).
- ⁴³ I. R. Klebanov, S. S. Pufu, and B. R. Safdi, *Journal of High Energy Physics* **2011**, 38 (2011).
- ⁴⁴ L. Fei, S. Giombi, I. R. Klebanov, and G. Tarnopolsky, *Journal of High Energy Physics* **2015**, 155 (2015).
- ⁴⁵ S. Giombi and I. Klebanov, *Journal of High Energy Physics* **2015**, 1 (2015).
- ⁴⁶ E. M. Stoudenmire, P. Gustainis, R. Johal, S. Wessel, and R. G. Melko, *Physical Review B* **90**, 235106 (2014).

- ⁴⁷ A. B. Kallin, E. M. Stoudenmire, P. Fendley, R. R. P. Singh, and R. G. Melko, *Journal of Statistical Mechanics: Theory and Experiment* **2014**, P06009 (2014).
- ⁴⁸ H. Casini and M. Huerta, *J. Phys.* **A42**, 504007 (2009).
- ⁴⁹ J. Helmes, L. E. Hayward Sierens, A. Chandran, W. Witczak-Krempa, and R. G. Melko, *Phys. Rev. B* **94**, 125142 (2016), 1606.03096.
- ⁵⁰ T. Hirata and T. Takayanagi, *Journal of High Energy Physics* **02**, 042 (2007).
- ⁵¹ P. Bueno, R. C. Myers, and W. Witczak-Krempa, *Phys. Rev. Lett.* **115**, 021602 (2015).
- ⁵² P. Bueno and R. C. Myers, *Journal of High Energy Physics* **1508**, 068 (2015).
- ⁵³ T. Faulkner, R. G. Leigh, and O. Parrikar, *Journal of High Energy Physics* **2016**, 1 (2016).
- ⁵⁴ S. Inglis and R. G. Melko, *New Journal of Physics* **15**, 073048 (2013).
- ⁵⁵ X. Chen, G. Y. Cho, T. Faulkner, and E. Fradkin, *Journal of Statistical Mechanics: Theory and Experiment* **2015**, P02010 (2015).
- ⁵⁶ W. Witczak-Krempa, L. E. H. Sierens, and R. G. Melko, *Cornering gapless quantum states via their torus entanglement* (2015), arXiv:1603.02684.
- ⁵⁷ L. Chojnacki, C. Q. Cook, D. Dalidovich, L. E. Hayward Sierens, É. Lantagne-Hurtubise, R. G. Melko, and T. J. Vlaar, *Phys. Rev. B* **94**, 165136 (2016), 1607.05311.
- ⁵⁸ H. Casini and M. Huerta, *JHEP* **03**, 048 (2009), 0812.1773.
- ⁵⁹ B. Swingle (2010), 1010.4038.
- ⁶⁰ K. Sun, H. Yao, E. Fradkin, and S. A. Kivelson, *Physical Review Letters* **103**, 046811 (2009).
- ⁶¹ C. A. Agón, M. Headrick, D. L. Jafferis, and S. Kasko, *Physical Review D* **89**, 025018 (2014).
- ⁶² M. A. Metlitski and T. Grover, *Entanglement entropy of systems with spontaneously broken continuous symmetry* (2011), arXiv:1112.5166.
- ⁶³ A. B. Kallin, M. B. Hastings, R. G. Melko, and R. R. P. Singh, *Phys. Rev. B* **84**, 165134 (2011).
- ⁶⁴ N. Shiba, *ArXiv e-prints* (2017), 1701.00688.
- ⁶⁵ R. E. Arias, D. D. Blanco, and H. Casini, *Journal of Physics A: Mathematical and Theoretical* **48**, 145401 (2015).
- ⁶⁶ P. Bueno and W. Witczak-Krempa, *Phys. Rev. D* **95**, 066007 (2017).
- ⁶⁷ T. Faulkner, *Journal of High Energy Physics* **2015**, 33 (2015).
- ⁶⁸ J. L. Cardy and I. Peschel, *Nuclear Physics B* **300**, 377 (1988).
- ⁶⁹ P. Bueno, R. C. Myers, and W. Witczak-Krempa, *Journal of High Energy Physics* **9**, 91 (2015).
- ⁷⁰ P. Calabrese and J. Cardy, *Journal of Physics A: Mathematical and Theoretical* **42**, 504005

(2009).

- ⁷¹ T. Grover, A. M. Turner, and A. Vishwanath, *Phys. Rev. B* **84**, 195120 (2011).
- ⁷² Z. Komargodski and A. Schwimmer, *Journal of High Energy Physics* **2011**, 99 (2011).
- ⁷³ A. H. Castro Neto and E. Fradkin, *Nuclear Physics B* **400**, 525 (1993).
- ⁷⁴ S. Sachdev, *Physics Letters B* **309**, 285 (1993).
- ⁷⁵ E. Elizalde, *Ten Physical Applications of Spectral Zeta Functions* (Springer, 2012), ISBN 978-3-642-29405-1.
- ⁷⁶ P. Di Francesco, P. Mathieu, and D. Sénéchal, *Conformal Field Theory* (Springer-Verlag, New York, 1996), ISBN 0-387-94785-X.
- ⁷⁷ H. Casini and M. Huerta, *Journal of Physics A: Mathematical and Theoretical* **42**, 504007 (2009).
- ⁷⁸ I. Peschel, *Journal of Physics A: Mathematical and General* **36**, L205 (2003).